



**UNIVERSIDADE ESTADUAL PAULISTA**  
**"JULIO DE MESQUITA FILHO"**  
**INSTITUTO DE GEOCIÊNCIAS E CIÊNCIAS EXATAS**



Trabalho de Formatura

Curso de Graduação em Geologia

STRONTIUM ISOTOPES MEASUREMENT FROM BUNKER CAVE SYSTEM: A CONTRIBUTION FOR  
THE MULTI-PROXY PALEOCLIMATE RESEARCH OF CENTRAL EUROPE

Cintia Fernandes Stumpf

Prof. Dr. Daniel Marcos Bonotto

Prof. Dr. Augusto Mangini

Rio Claro (SP)

2013

UNIVERSIDADE ESTADUAL PAULISTA  
Instituto de Geociências e Ciências Exatas  
Câmpus de Rio Claro

*CINTIA FERNANDES STUMPF*

STRONTIUM ISOTOPES MEASUREMENT FROM  
BUNKER CAVE SYSTEM: A CONTRIBUTION FOR THE  
MULTI-PROXY PALEOCLIMATE RESEARCH OF  
CENTRAL EUROPE.

Trabalho de Formatura apresentado ao  
Instituto de Geociências e Ciências  
Exatas - Câmpus de Rio Claro, da  
Universidade Estadual Paulista Júlio de  
Mesquita Filho, para obtenção do grau de  
Geólogo.

*Rio Claro - SP*  
2013

551.44 Stumpf, Cintia Fernandes  
S934s Strontium isotopes measurement: a contribution for the  
multi-proxy paleoclimate research of Central Europe / Cintia  
Fernandes Stumpf. - Rio Claro, 2013  
64 f. : il., figs., tabs.

Trabalho de conclusão de curso (Geologia) - Universidade  
Estadual Paulista, Instituto de Geociências e Ciências Exatas  
Orientador: Daniel Marcos Bonotto  
Coorientador: Augusto Mangini

1. Speleology. 2. Epikarste. 3. Strontium isotope ratio. 4.  
Speleothem. 5. Karst water. 6. Weathering. 7. Soils. I. Título.

*CINTIA FERNANDES STUMPF*

STRONTIUM ISOTOPES MEASUREMENT FROM  
BUNKER CAVE SYSTEM: A CONTRIBUTION FOR THE  
MULTI-PROXY PALEOCLIMATE RESEARCH OF  
CENTRAL EUROPE.

Trabalho de Formatura apresentado ao  
Instituto de Geociências e Ciências  
Exatas - Câmpus de Rio Claro, da  
Universidade Estadual Paulista Júlio de  
Mesquita Filho, para obtenção do grau de  
Geólogo.

Comissão Examinadora

Augusto Mangini, Prof. Dr. at Heidelberg University

Amauri Antônio Menegário, Prof. Dr. at UNESP University

Leticia Hirata Godoy, Prof. MSc. at UNESP University

Rio Claro, 28 de Junho de 2013.

Assinatura do(a) aluno(a)

assinatura do(a) orientador(a)

Dedicated to my family...

## ACKNOWLEDGEMENTS

I am really grateful to the people who assisted me during this first scientific journey, particularly to Andrea Schröder-Ritzrau for the constructive reviews and Augusto Mangini for the opportunity to realize my Bachelor these in Umweltphysik Institute, Heidelberg/Germany. I would like to thank René Eichstädter for the long German classes and also the technical approach, Sylvia Riechelmann for the field excursions to Bunker cave. This project would not be done without the support from DAPHENE research group.

I also thank Professors Peter Hackspacher and Ulrich A. Glasmacher, coordinators from the DAAD/CAPES exchange program between Brazil and Germany. It was a pleasure and a wonderful experience to study in Germany for a year and use the analytical facilities of Heidelberg University. Finally I thank Maria Luiza de Carvalho Ferreira for the constructive discussions.

## ABSTRACT

In recent years speleothem has been intensely studied due to its great potential of registering paleoclimate proxies but some considerably uncertainties regarding speleothem proxy interpretation still exist. In order to minimize these uncertainties, multi-proxy approach has been used. Here is presented the strontium isotope record from Bunker cave, northwest Germany. This cave was previously studied and has proved well record paleoclimate changes during Holocene for central Europe.  $^{87}\text{Sr}/^{86}\text{Sr}$  ratio is presented for rain water, A-horizon soil (water and leachate), C-horizon soil (water and leachate), host rock and host rock leachate, drip water and from a stalagmite (Bu4) previously dated covering the Holocene. Upper soil presented the higher values in contrast with host rock (lower values). Drip water and C-horizon presented intermediated ratios. Sr isotopes are used to track the source of  $^{87}\text{Sr}/^{86}\text{Sr}$  in the Bunker system, resulting in a mixture between A-horizon soil, C-horizon soil and host rock. A decreasing trend in Bu4 indicates change in the Sr source in the system.

**Keywords:** Strontium isotope ratio. Speleothem. Karst water. Soils. Weathering.

## RESUMO

Nos últimos anos espeleotemas tem sido intensamente estudados devido ao seu grande potencial de registro de proxies paleoclimáticas, mas ainda existem algumas incertezas consideráveis em relação à interpretação das proxies em espeleotemas. A fim de minimizar estas incertezas, aproximação multi-proxy tem sido utilizada. Aqui é apresentado o registro isótopos de estrôncio da caverna Bunker, noroeste da Alemanha. Esta caverna foi previamente estudada e provou registrar bem mudanças paleoclimáticas durante o Holoceno na Europa central. Razão de  $^{87}\text{Sr}/^{86}\text{Sr}$  é apresentada para a água da chuva, horizonte A do solo (água e solução lixiviada), horizonte C do solo (água e solução lixiviada), rocha hospedeira e lixiviado da rocha, água de gotejamento e de uma estalagmite (Bu4) previamente datada, cobrindo o Holoceno. O solo orgânico apresentou os valores mais elevados, em contraste com a rocha hospedeira (valores de razão menores). Água de gotejamento e horizonte-C do solo apresentaram índices intermediários. Isótopos de Sr são utilizados para rastrear a fonte de  $^{87}\text{Sr}/^{86}\text{Sr}$  no sistema Bunker, resultando em uma mistura entre o horizonte A do solo, horizonte C do solo e rocha hospedeira. Uma tendência descendente na Bu4 indica mudança na fonte de Sr no sistema.

**Palavras-chave:** Razão isotópica de estrôncio. Espeleotemas. Água cárstica. Solos. Intemperismo.

## List of Figures

Figure 1 - Location of Bunker cave. The European continent/ Germany / North Rhine-Westphalia state / Bunker Cave.....	15
Figure 2 - Geological map of the Rhenish Slate Mountains. ....	18
Figure 3 - The comprehensive karst system .....	23
Figure 4 - The curve of $^{87}\text{Sr}/^{86}\text{Sr}$ versus geologic time.....	27
Figure 5 -Fractioning correction normalizing the measured ratio to a fixed absolute $^{88/86}\text{Sr}$ value .....	30
Figure 6 - Survey map of the monitoring chambers of Bunker Cave and longitudinal profile of the cave .....	32
Figure 7 - Acid dependency of $k'$ for various ions at 23-25°C. ....	34
Figure 8 - Bu4 stalagmite, with the depth of samples made.....	35
Figure 9 - Flowchart representing the chromatographic column process for separating Sr .....	37
Figure 10 - Distribution of ratio values from different source samples.....	40
Figure 11 - Synthesis diagram with the minimum, maximum and mean values of $^{87}\text{Sr}/^{86}\text{Sr}$ ratio. ....	41
Figure 12 - Soil water samples .....	42
Figure 13 - $^{87}\text{Sr}/^{86}\text{Sr}$ from soils leachates and total digestion .....	43
Figure 14 - HR $^{87}\text{Sr}/^{86}\text{Sr}$ ratios. ....	44
Figure 15 - $^{87}\text{Sr}/^{86}\text{Sr}$ ratio for Bu4 stalagmite.....	45
Figure 16 - Comparison between $^{87}\text{Sr}/^{86}\text{Sr}$ ratio from stalagmite and drip water.....	45
Figure 17 - Mixing lines. In the right it is plotted the Sr ratios of the analyzed samples. ....	48

## List of Tables

Table 1 - The four strontium isotopes, their masses and relative abundance in nature. ....	28
Table 2: Summary of the samples used in this study, all related to Bunker Cave System. ....	32
Table 3 - Flowchart differing the solid and fluid phases and the sequential stacking materials analyzed, as well as the mean value of its $^{87}\text{Sr}/^{86}\text{Sr}$ ratios. Notice the lower ratio value for the HR. ....	39

## **LIST OF ABBREVIATIONS AND ACRONYMS**

<b>Bu4</b>	Stalagmite
<b>BuS</b>	Bunker cave soil
<b>DW</b>	Drip Water
<b>HR</b>	Host rock
<b>MS</b>	Mass Spectrometry
<b>MW</b>	Meteoric Water
<b>PCP</b>	Prior Calcite Precipitation
<b>REE</b>	Rare Earth Elements
<b>RW</b>	Rain Water
<b>SW</b>	Soil Water
<b>TD</b>	Total Digestion
<b>TIMS</b>	Thermal Ionization Mass Spectrometry

## SUMMARY

<b>1.0 INTRODUCTION .....</b>	<b>12</b>
<b>1.1 Stalagmite as paleoclimate proxy .....</b>	<b>12</b>
<b>1.2 General setting of the Bunker Cave and Related Environment .....</b>	<b>13</b>
1.2.1 Access and Location .....	15
1.2.2 Soil, Vegetation and Climate.....	15
1.2.3 Geology and Geomorphology.....	17
1.2.4 Geology of the Cave .....	19
<b>2.0 OBJECTIVES.....</b>	<b>21</b>
<b>3.0 THEORETICAL BACKGROUND.....</b>	<b>22</b>
<b>3.1 Aspects on Karst Science .....</b>	<b>22</b>
3.1.1 Karst system and Karst Hydrogeology.....	22
3.1.2 Speleothems.....	25
<b>3.2 Aspects on Isotopic Analyses .....</b>	<b>26</b>
3.2.1 Isotopic data on paleoclimate and environmental science.....	26
3.2.2 The Strontium Isotopes .....	28
<b>4.0 METHODOLOGY.....</b>	<b>31</b>
<b>4.1 Source of the Samples .....</b>	<b>31</b>
<b>4.2 Equipment.....</b>	<b>33</b>
<b>4.3 Reagents .....</b>	<b>33</b>
<b>4.4 Procedure.....</b>	<b>34</b>
4.4.1 Rock Samples preparation.....	34
4.4.2 Soil Samples preparation.....	35
4.4.3 Water Samples preparation.....	36
<b>4.5 Chemistry process.....</b>	<b>36</b>
<b>4.6 Mass spectrometry analyses .....</b>	<b>37</b>
<b>5.0 RESULTS .....</b>	<b>39</b>
<b>5.1 Rain Water.....</b>	<b>41</b>
<b>5.2 Soil water and soil leachates .....</b>	<b>41</b>
<b>5.3 Host Rock.....</b>	<b>43</b>
<b>5.4 Stalagmite and Drip Water .....</b>	<b>44</b>
<b>6.0 DISCUSSION.....</b>	<b>46</b>

<b>7.0 CONCLUSIONS.....</b>	<b>53</b>
<b>REFERENCES.....</b>	<b>55</b>
<b>BIBLIOGRAPHY .....</b>	<b>58</b>
<b>APPENDIX A – SAMPLE LIST.....</b>	<b>59</b>
<b>ANNEX A – BU4 DATING DATA .....</b>	<b>63</b>

## 1.0 INTRODUCTION

### 1.1 Stalagmite as paleoclimate proxy

Proxies are any parameters that can be measured in an archive and which stand in, or substitute for an environmental variable (FAIRCHILD and BAKER, 2012). To high-resolution climate proxy, it is understood monthly to decadal resolution, that can be obtained from lake or marine sediments, speleothems, ice cores, corals, tree rings and also human archive from documentary records (COBB et al 2008). Monthly to annually resolved speleothem proxy records are still extremely rare (FLEITMANN et al 2008). Speleothems (stalagmites, stalactites and flowstones) as proxy is a recent resource for paleoclimate investigation.

With the increase interest on speleothems in science due to the potential to new studies and interpretation in the environmental changes, Fairchild and Baker (2012) attempt to concentrate the knowledge on the theme, clarifying, among other topics, the preferential use of stalagmite as a paleoclimate proxy among other speleothems (described below).

First, stalagmites may be precisely dated. The development of techniques for precise and accurate U-Th dating on small amounts of sample (each sedimentation layer) is the most important factor that has allowed speleothem science to become so prominent in recent years. The main principle is that during speleothem growth, it incorporates some uranium from aqueous solution, but fails to incorporate the insoluble element thorium. The nuclide  $^{230}\text{Th}$  accumulates over time, by alpha-decay from  $^{234}\text{U}$ , after that particular speleothem growth layer has been deposited. The half-life of  $^{234}\text{U}$  is around 245.000 years and  $^{230}\text{Th}$  around 75.400 years.

Another point might be the substantial contribution of the last decade research to paleoclimate records that placed speleothems at the forefront of paleoenvironment reconstructions (FLEITMANN et al 2008), despite the great uncertainty that is often present. As speleothems contain several proxy parameters that can be used singly or in combination, multiple proxies are being developed to better understand the climatic changes. It may be more effective for our comprehension the use of multi-proxy approaches available on stalagmites to reduce the uncertainties.

Finally, stalagmites may record continuous episodes of growth that can present thousand years in duration. The calm and stable environment of a cave contribute for

the preservation of information, different from other proxies in which the information can be lost due e.g. to erosion or bioturbation. Speleothems are also widespread in inhabited continental areas, principally in northern hemisphere where large carbonate areas present karstic regions with stalagmites recording the continental past climate. This kind of rock is also physically and chemically robust, contributing to collection and laboratory procedure.

## **1.2 General setting of the Bunker Cave and Related Environment**

Bunker cave was discovered in 1926 during road works, but only in 1989 the deeper parts of the cave were explored by opening a narrow crevice. The entrance area is artificially enlarged due to its use as an air-raid shelter during the second World War. It is an intensively studied karst area (NIGGEMANN et al., 2008; NIGGEMANN et al., 2003; DREYER et al., 2008), one of the reasons for the choice of this cave for the paleoclimate studies (RIEHELMANN et al. 2011). A gate protects the little entrance (with an approximated dimension of 1m X 60 cm) nearby the road, offering an easy accessibility during all year's period.

The cave has a central European location (see item 1.2.1), in the so called Rhenish Slate Mountains, NW Germany, and it is part of a 3,5km long cave system with Emst cave. They are connected by a narrow and impassable cleft. The cave system is inserted in a 700 meter thick Middle to Upper Devonian limestone unit, composed by low-Mg limestone hosting thin dolomite veins. The thickness of the host rock above the cave ranges from 15 to 30m (FOHLMEISTER et al., 2012).

The Sauerland, region where Bunker cave is inserted, is a hilly area spreading across most of the southeast part of North Rhine Westphalia Bundesland. It is today an important touristic region, in particular for outdoor sports and scenic recreation. It is limited in west by the Bergische Land, to the south by Siegerland, to the north by Haarstrang and Hellwegzone and to the east by Bergland (Waldecker Land) (fig. 1). The major rivers of the Sauerland are the Ruhr and Lenne rivers (BAALES et al, 2011).

Over a large surface of the Sauerland carbonate rocks are exposed, in which numerous caves are typically found (BAALES et al, 2011). According to the same author, these caves present a special role in the history of research on different periods from

prehistory and also of archaeological research, since the first findings of human prehistory have been developed for central Europe.

In present days the cave is above the groundwater level however it still an active cave with percolation of meteoric water. From the monitoring data (RIECHELMANN et al., 2011), it presents a mean air cave temperature of 10,6°C and a mean value of cave air humidity of 93%.

Four stalagmites (Bu1, Bu2, Bu4 and Bu6) were sampled in the cave, of which only Bu4 is used in this study. All the four stalagmite data represent a partly overlapped time series covering the last 10,8ka BP, almost the entire Holocene epoch, and present proxy signals that are comparable with other isotope records and seems to be representative for central European Holocene climate variability (FOHLMEISTER et al. 2012).

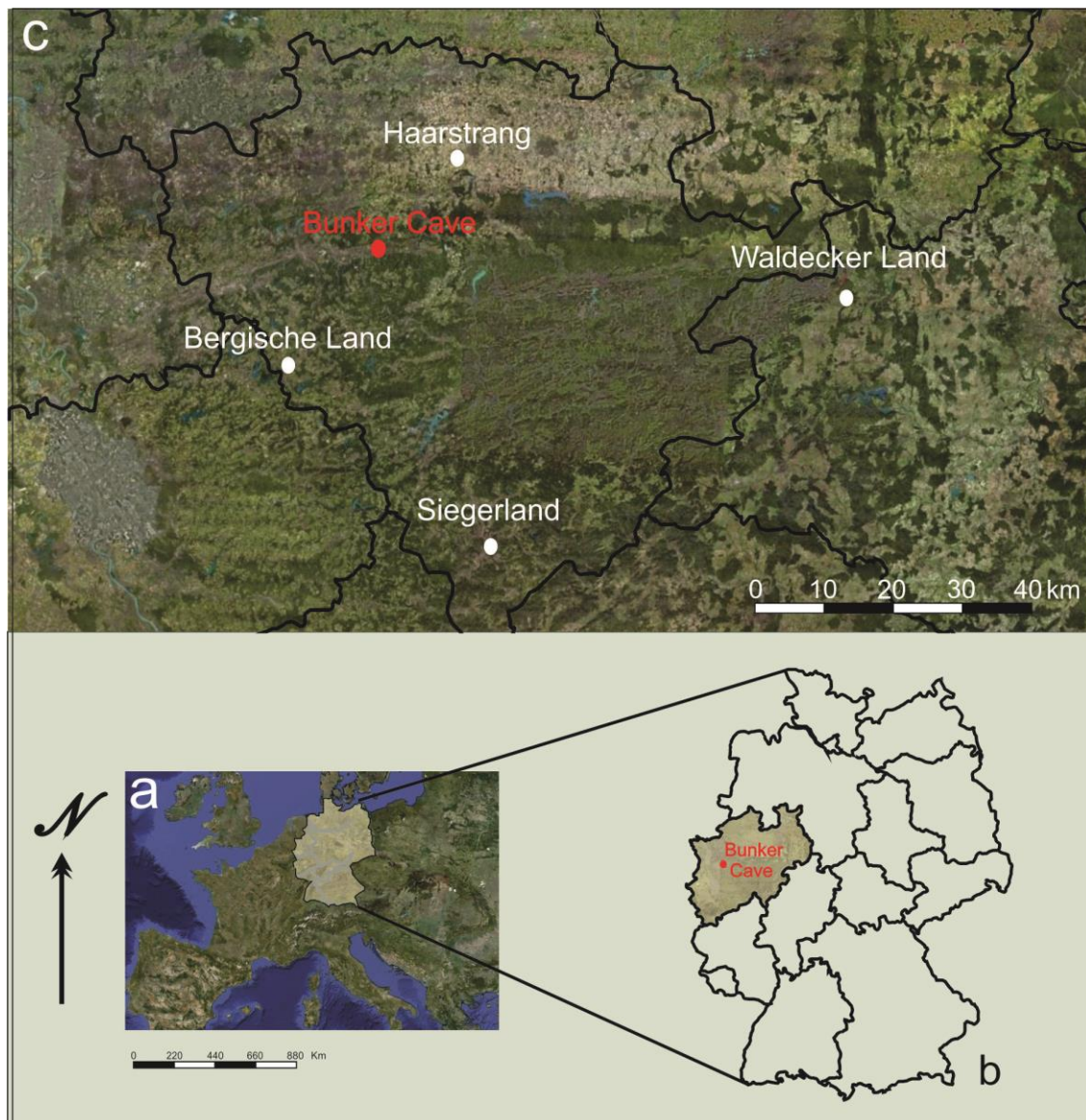


Figure 1 -Location of Bunker cave. a) The European continent featured Germany boundary, in the central European region; b) limits of Germany. The North Rhine-Westphalia state is highlighted and Bunker Cave location is indicated; c) a detailed view on the North Rhine-Westphalia state, showing the limits of Sauerland region and the position of Bunker Cave in relation to the geologic context of Rhenish Slate Mountains. Source: Google Earth image. Assessed in 15.04.2013.

### 1.2.1 Access and Location

Bunker Cave is located on the Rhenish Slate Mountains, western part of Germany (Sauerland), central Europe, exactly in Iserlohn city. The biggest and reference city nearby is Dortmund. The entrance of the cave (fig. 1) is in the coordinate 51°22'03' N ; 7°39'53' E, 184 m above sea level on a south dipping hill slope of the DröschederEmst, a small karst plateau with approximately 1Km<sup>2</sup> (RIECHELMANN et al. 2011).

The Sauerland region can be reached by car or train. By car, the drive should be either via the E37 road from Cologne or via E30 road from Berlin (capital). From Dortmund, the largest city in the Ruhr Area, approximately 35 Km from Iserlohn, it is possible to reach Iserlohn by via E41. By train, it is reachable by Regional Express 16 (Essen – Hagen – Letmathe - Iserlohn - Siegen), Regional Bahn 53 (Iserlohn – Schwerte - Dortmund) or either Regional Bahn 91 (Hagen – Letmathe – Iserlohn – Siegen). The closest commercial airport is Dortmund Airport.

### 1.2.2 Soil, Vegetation and Climate

The formation of soil during the Holocene in the Rhenish Massif depends largely on the vertical sequence of Pleistocene periglacial slope deposits and on the degree of alteration of the underlying slates (SAUER& FELIX-HENNIGSEN, 2006). The soil profile above the cave has up to 70 cm thick (see fig. 6) and consist of a weathered material from the limestone host rock and loess/debris deposits from Pleistocene epoch.

The limestone surface is covered by brown and loamy soil (inceptisol/alfisol developed from loess loam). A thin humic A-horizon with less than 10 cm thick covers a brown/yellow B-horizon, which originated from loess loam and frequently contains limestone fragments. The C-horizon consists of the massive limestone, the host rock (FOHLMEISER et al. 2012).

Inceptisols are soils of semiarid to humid environments that generally exhibit only moderate degrees of soil weathering and development. This kind of soil has a wide range in characteristics and occurs in a wide variety of climates. It makes up about 17%

of the world's ice free land surface. In other hand, an alfisol is in semiarid to moist areas. These soils result from weathering processes that leach clay minerals and other constituents out of the surface layer and into the subsoil, where they can hold and supply moisture and nutrients to plants. They were formed primarily under forest or mixed vegetative cover and are productive for most crops. It makes up about 10% of the world's ice-free land surface (NRCS, 2013).

The soil water present a alkali pH of 7,6. Part of the CO<sub>2</sub> in the soil air is dissolved in the soil water, promoting the acidification of the water. The vegetation above the cave consists mainly in a mixture of deciduous forest (mainly ash and beech trees) and scrub.  $\delta^{13}\text{C}$  values indicates C<sub>3</sub> vegetation, including bushes and trees in the temperate climate zone (RIECHELMANN et al. 2011).

Ehleringer&Cerling (2002) use the term C<sub>3</sub> vegetation not just as a metabolism classification but also as an approach of description of plant environment according to its carbon metabolism pathways. The ancestral pathway for carbon fixation made by C<sub>3</sub> plants may be related to the [CO<sub>2</sub>]/[O<sub>2</sub>] ratio establishing a strong link between current atmospheric conditions and photosynthetic activity.

The C<sub>3</sub> photosynthesis is described by Ehleringer&Cerling (2002) as a multi-step process in which the carbon from CO<sub>2</sub> is fixed into stable organic products. This occurs by the combination of Rubisco (a 5C molecule) with CO<sub>2</sub> to form two molecules of phosphoglycerate (3C molecule). However, Rubisco is an enzyme capable of catalyzing two distinct reactions depending on the substrate. When CO<sub>2</sub> is the substrate, lead the formation of two molecules of phosphoglycerate (3C molecule), in contrast when O<sub>2</sub> is the substrate, lead the formation of just one phosphoglycerate plus one phosphoglycolate (2C molecule).

This reaction results in less carbon fixation and lead the production of CO<sub>2</sub> in a process known as photorespiration. For the authors, the consequence of rubisco sensitivity to O<sub>2</sub> is that the efficiency of the C<sub>3</sub> photosynthesis decreases as atmospheric CO<sub>2</sub> decreases, it is to say, under elevated CO<sub>2</sub> environments or at cool temperatures, C<sub>3</sub> vegetation shows a great efficiency of photosynthesis.

In relation to climate, the cave microclimate is much more homogeneous and constant than the outside climate. Riechelmann (2011) discusses the slightly seasonal variation

of Bunker Cave air  $p\text{CO}_2$  as a result of inside/outside differences in temperature. When the outside air temperature is lower than the cave temperature (during winter), the warmer and less dense cave air ascends and leaves the cave through the upper entrance. This leads to cold surface air being sucked into the cave through the lower entrance. The opposite phenomenon is observed when the surface temperature is higher than the cave temperature (during summer). This phenomenon generates ventilation in the cave, decreasing the  $p\text{CO}_2$  from cave air, principally in winter. It is important to note that the seasons in the northern hemisphere (Europe) are distinct from the southern hemisphere (Brazil). In Europe summer occurs from Jun to August and the winter December/January/February.

### 1.2.3 Geology and Geomorphology

The Rhenish Slate Mountains, at the western boundary of Germany, was palaeogeographically part of the Cornwall-Rhenish Basin, which was characterized by a back-arc extension and rapid subsidence during the Late Devonian and earliest Carboniferous and it is part of the Variscan mountain belt in Central Europe (FRANKE, 2000). The uppermost Devonian of the basin is characterized by the interruption of pelagic conodont biofacies, which is replaced by a more nearshore biofacies. These faunal changes, associated with deep lithological changes elsewhere in Europe, are thought to be the result of some kind of Devonian/Carboniferous event, characterized by the extinction of many fossil groups and with a subsequent rapid diversification of the others that survived the event (STEENWINKEL, 1992). A geological map of the area is shown in fig. 2.

The rock uplift of the region, locally accompanied by volcanic activity to the south occurred in a prolonged period during the early Tertiary, according to Meyer; Hetzel; Strauss, (2010) due to isostatic response of the lithosphere heating by a mantle plume located beneath the Eifel Region.

Geomorphologically, it consists predominantly of Devonian slates and siltstones, forming extensive elevated plateaus. Under warm-humid conditions of the Upper Mesozoic and Lower Tertiary, intensive weathering led to formation of a planation surface covered by thick saprolites and kaolinitic soils. During Pleistocene glaciations, the area experienced periglacial conditions that resulted in erosion of the soils and parts of the saprolites and also dissected the flated surfaces forming the actual elevated

plateaus (SAUER& FELIZ – HENNINGSEN, 2006). Modern soils are developed above Pleistocene periglacial slope deposits.

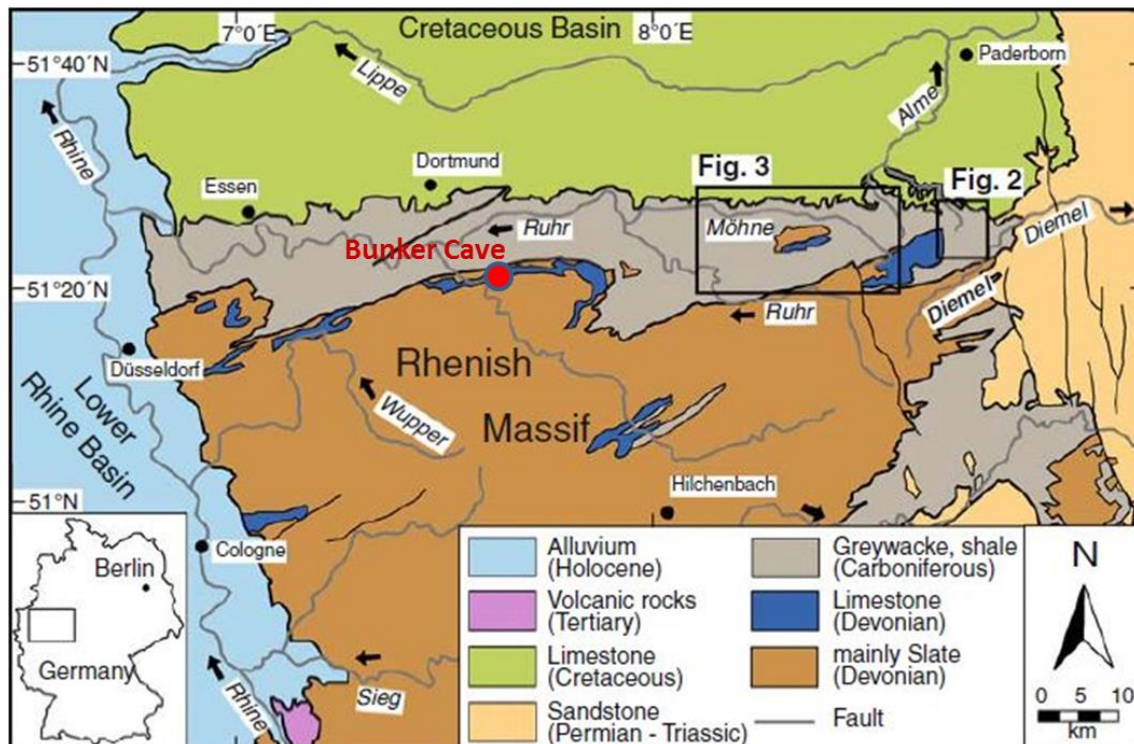


Figure 2 - Geological map of the Rhenish Slate Mountains. The black line between mainly slate Devonian rocks and the greywacke, shale carboniferous rock represent the important Devonian/carboniferous event. A discontinuous belt of submarine “shoals” formed by Givetian-Frasnian reef masses is represented in blue. Source: Meyer et al., (2010).

During the Upper Carboniferous period, the sediments were folded by the Variscan orogeny, bordered to the north against the autochthonous foreland along the Variscan front (HEIN, 1993). Tectonic uplift, which occurred during the mid-Tertiary, led to the development of the Rhine graben, which crosses the Rhenish Massif from southeast to northwest (SAUER& FELIZ – HENNINGSEN, 2006). Apart from slates and siltstones, there is also present some graywacke, quartzite and limestone. The rivers dissect intensely these units, forming reliefs dominated by steep valleys. Away from the river's edge planation surfaces characterize the landscape. More competent rocks, such as quartzite, follow the general direction of the Variscan orogeny, striking in southwest to northeast direction.

Widespread frost cracks associated with sand wedges are interpreted by Sauer & Feliz – Henningsen (2006) as a result of ice lens formations indicating the action of cold climate in the region. The long-distance mass transport in the weak inclination slopes of

the Massif, also suggest the process of gelifluction. Frost creep and gelifluction are the cold-climate representatives of mass-wasting processes.

Sauer & Felix-henningsen (2006) present a reconstruction of the climate and landscape history of the Rhenish Massif since the Mesozoic. Subtropical to tropical conditions indicated by the thick saprolite cover led to intensive deep weathering with the formation of kaolinitic soils and saprolites from slates and siltstones. Erosive denudation occurred simultaneously, developing planation surfaces. The warm and humid conditions continued until the end of the Miocene and came back in several phases during the Pliocene, but, besides these warm phases, the Pliocene was in general characterized by an overall temperature decrease marking the transition from interglacial to glacial period (Tertiary – Pleistocene).

The Rhenish Massif was not glaciated during the Pleistocene, however it was subject to periglacial conditions. In this Epoch, the rivers incised deeply into the basement rocks, dissecting the planation surfaces. Extensive erosion occurred by the congelifraction, gelifluction and melt water runoff processes. Above the remnants of the Mesozoic – Tertiary surface were formed the Pleistocene Periglacial slope deposits (SAUER & FELIZ – HENNINGSEN, 2006). Eolian deposition forming loess deposits, took place during cold and dry periods in the Middle and Upper Pleniglacial, but subsequently more humid conditions allowed gelifluction of the loess layers. With the end of the last ice age the landscape was stabilized and no significant slope processes occurred until historical time, when deforestation and agricultural land use again led to favorable conditions for extensive erosion.

#### 1.2.4 Geology of the Cave

The cave is developed in Devonian limestone, represented in blue in the geological map (fig. 2). This carbonate unit occurs as lenses following the boundary between the Devonian and Carboniferous rocks.

As it can be suggested observing fig. 6, the fractures are oriented predominantly NNW-SSE, controlling the development of the cave conduits. Occasionally this family of fractures can host thin dolomite veins. The fractures dip direction is mainly towards SW with an angle between 30 and 80 grads (RIECHELMANN et al. 2011).

The cave presents actively drip sites with growing speleothems, e.g. Bu4 stalagmite, studied in this coursework, sampled in an actively drip site. According to the monitoring data (RIECHELMANN et al. 2011), the drip-rate patterns of most drip sites are consistent with the main infiltration events, taking into account a delay of several months. An instantaneous response to precipitation is not observed for any drip site indicating a specific water capacity threshold in the soil/karst aquifer.

The karst aquifer recharge water seems to be well mixed from the uniform drip water  $\delta^{18}\text{O}$  data. The water percolating through the soil and host rock is stored, and the drip sites document seepage flow from these reservoirs with an average residence time of up to few years (RIECHELMANN et al. 2011). The velocity of seepage flow (the slow movement of water through a porous surface) is determined by the permeability of the respective geological unity and the unsaturated soil.

No impermeable formations such as shales are present above the cave and the Devonian limestone is in outcrop in the surface. As the cave is above the actual water base level, no river flow through the cave, similar to the Belgian Père Noël cave (VERHEYDEN et al, 2000), meaning that the water in the cave system is restricted to autogenic input (meteoric water) percolating directly downwards through the overlying soil and fresh limestone.

## **2 OBJECTIVES**

The aim of this scientific work is to correlate different types of samples from exokarst, epikarst and endokarst, focusing on the process that occur with the isotopic signal of Sr between the original signal in surface and the final signal registered in speleothems in sub-surface, objecting to track how karst water composition is modified in its environmental context. The samples are: one dated stalagmite covering entire Holocene (FOHLMEISTER, 2012), meteoric, soil and drip waters of the cave system, host rock and soil of different horizons. It is also an objective to determine the isotopic geochemistry of strontium in Bunker cave and analyze which are the variables that may influence this specific isotopic system.

### 3 THEORETICAL BACKGROUND

#### 3.2 Aspects on Karst Science

Kranjc (2001) explains the international term “karst” as derived from a karst plateau in the background of Trieste bay, in the Adriatic sea, by the border between Slovene and Italian. This region is known as Kras in Slovenia and consists of Cretaceous and Tertiary carbonate rocks, with well-developed underground water flow systems. In this way, “Kras” is translated into Karst in German, Carso in Italian and Carste in Portuguese language. The author also refers the meaning of the prefix kras as stone, and relates it to the first known ethnic groups living on the nowadays Slovenian territory, named Carni. This Kras region was the first intensively studied karst terrain, and thereafter similar places were referred also as karst when presented same characteristics, as a reference to the Slovenian landscape, an international term used until today.

##### 3.2.1 Karst system and Karst Hydrogeology

Ford & Williams (1996) define karst as a distinctive hydrology terrain where landforms arising from a combination of high rock solubility and well developed secondary porosity. Another typical feature is the development of unusual subsurface hydrology. A variety of forms, either in surface and subsurface, characterize karst regions, such as dolines, karren, poljes and caves (WAELE et al, 2009). Those distinctive landforms are typical of karst landscapes and are formed by solution along pathways provided by the structure, reinforcing the idea that just solubility of the rock alone is insufficient to produce karst, therefore bedding planes, joints and faults have also an important paper in controlling pathways of underground flow (FORD& WILLIAMS, 1996).

Karst environment or karst-like landscapes can be formed in different lithologies, such as quartzites, sandstone, granites (MONTEIRO& RIBEIRO, 2001; HARDT et al 2010; AUBRECHT et al, 2011; WRAY, 1999; GONÇALVES et al., 2011; RODRIGUEZ, 2003) however carbonate rocks are the most common lithotype to karst development. These rocks are more abundant in the northern hemisphere in comparison to Gondwana continents that present some carbonate of cretaceous or later age related to post-breakup of the super-continent (FORD& WILLIAMS, 1996).

A systematic view of karst was proposed by Ford &Willians (1996), where the recharge areas are the input on the system, the caves and karstic aquifer where the transformations take place and finally the springs representing the output of the system.

To understand carbonate karstified aquifer it is required to analyze the in-out put with a systematic understanding so that the intermediated process may be understood. A synthesized view is given in fig. 3.

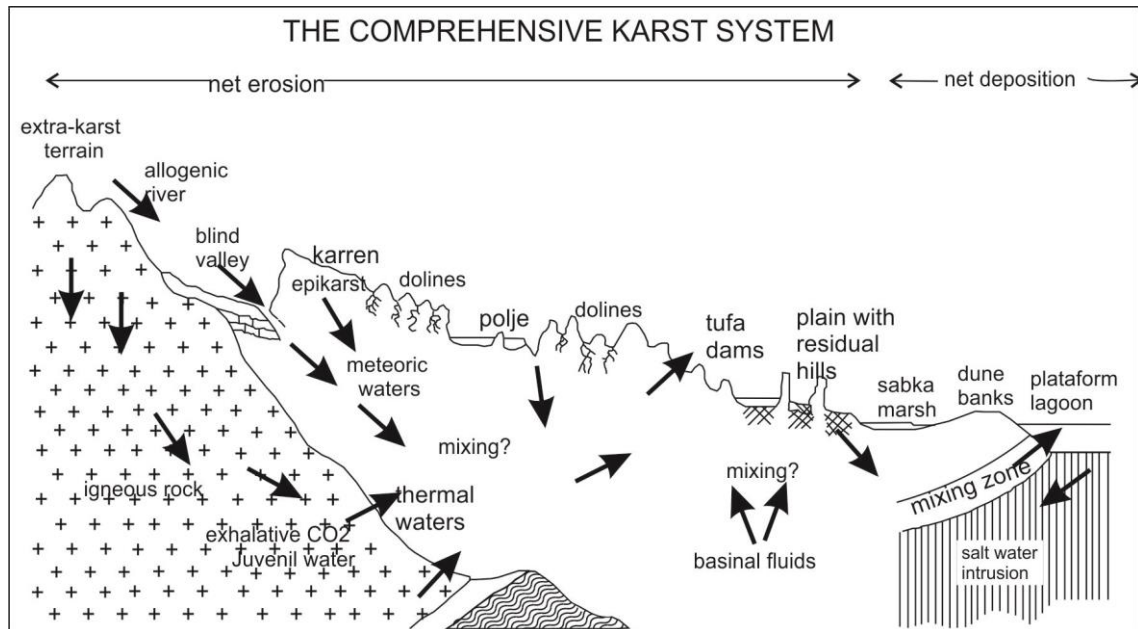
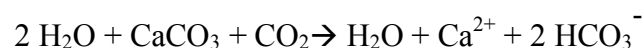


Figure 3 - The comprehensive karst system: a composite diagram illustrating the major phenomena encountered in active karst terrains. Source: Ford & Williams, (1996).

Caves are one of the most significant subsurface karst features, principally because of the possibility of being explored and directly studied by us. They are empty spaces under the surface with an entrance connecting the underground with the surface where man can enter. Davis (1931) reinforces two contrasted processes that happen inside caves, excavation and replenishment. The solution work of percolating water associated with the corrosion potential promotes excavation processes, creating caves and generating the enlargement of the cavities. Following these conduits, the water concentrates and flows similarly to a surface drainage system. The saturated waters when exposed to e.g. lower carbon dioxide pressures may provoke calcite precipitation thus reestablishing chemistry equilibrium (replenishment process).

Karstification is the dissolution of the carbonate rock due to percolation of acidic water, following the reaction:



The addition of CO<sub>2</sub> from atmosphere and soil into meteoric water is responsible for the acidity of percolating waters, due to formation of the weak carbonic acid. The concentration of dissolved CO<sub>2</sub> is driven by both the temperature and CO<sub>2</sub> partial pressure of the atmosphere related to ground-water.

According to Waele et al. (2009), the dissolution, although much more powerful at the surface, continues underground slowly enlarging fissures and initial openings, forming the karst conduit system. Speleogenesis is the term for the whole evolution of karst systems, from the origin to their full development up to the present form. White (2002) assumes dissolution as a very rapid process on a geologic time scale, modifying constantly the flow paths. As a result, karst aquifers must be regarded as works in progress, due to its rapidly changing.

Generally climate is considered as a driving karst processes (BAKALOWICZ, 2005) because of its influence on triggering chemical reactions of dissolution and weathering, i.e. amount of precipitation, pCO<sub>2</sub> and hydraulic gradient (difference in elevation between the top of the karst recharge area and the spring base level).

In a geologic concept, Davis (1931) describes a continuous evolution of the landscape where excavation and replenishment process inside the cave happens simultaneously with tectonic uplift, lowering of the groundwater level, and surface erosion. In this case, surface karst features as dolines can reach cave roofs, opening this underground environment, and erosion might transform them to open or blind valleys with the removal of the walls. In geological time scale this may become eventually a new featureless peneplain surface and caverns will have vanish by erosion.

In a hydrological point of view, the water pathway through discontinuities from recharge area to spring creates a very high heterogeneity in the karst aquifer (BAKALOWICZ, 2005) with different length, size, direction conduits. This heterogeneity progressively becomes organized and hierarchizes in the same way as fluvial systems. The similarity with surface flows and not inter-porous flow is characteristic from karst aquifers. Karst hydrology requires a mix of surface water concepts and ground water concepts to be understood (WHITE, 2002).

Klimchouk (2000) define epikarst as the uppermost weathered zone of carbonate rocks with substantially enhanced and more homogeneously distributed porosity and

permeability, as compared to the bulk rock below. Its principal functions are to store and temporally distribute autogenic infiltration recharge to vadose zone. For Bakalowicz (2005) it may be compared to the skin of the karst, and exchange zone between the bio-atmosphere and the karst itself, storing groundwater where  $\text{CO}_2$  is produced and transported in solution and also where an air-soil-rock-water mixing occurs. Because of temporally storage in the epikarst (also called subcutaneous zone) diffuse infiltration water may require days to weeks to reach the water table. In contrast, where soils are thin and the bedrock is highly fractured, diffuse infiltration reaches the subsurface rapidly, giving sharp and peaked hydrographs that lag only slightly behind the precipitation (WHITE, 2002).

### 3.2.2 Speleothems

The word Speleothem comes from the Greek meaning *Spelaion* = cave and *Thema* = deposit. They represent the chemical sedimentation inside a cave, and are mainly composed by calcite or aragonite. Commonly present in mature cave systems, the dripstones are formed by the ions in solution transported by the drip water that comes from the epikarst/soil and drip from the cave roof causing mineral precipitation. During the first stages of active cave opening and enlargement, when fractures are occupied by streams and the cave found itself under the vadose zone, speleothem formation is inhibited.

Stalactites (from the Greek: *Stalaktós* = dripping) are the formations hanging from the cave roof. The solution in contact with the cave atmosphere (that present lower  $\text{pCO}_2$  than the water) degasses liberating  $\text{CO}_2$  to the cave air, causing the precipitation of calcite ( $\text{CaCO}_3$ ) that is not soluble in water. The rest of the drip follow the gravitational path downward to the cave floor to form the stalagmite (from the Greek: *Stalagmós* = dropping). The impact of the drip with the floor also provokes the degassing of the solution and consequently precipitation of calcite.

Stalagmites are especially used in paleoclimate research. Fairchild and Baker (2012) explain it due to the simple internal structure from stalagmite in comparison to stalactite or other speleothems (helictite, flowstone, cave pearls, etc.). Other characteristic is the clear internal layering from different time periods. Following the stalagmite axis it is possible to create time-series precisely dated and interpret according to the differences in the proxies parameters.

### 3.3 Aspects on Isotopic Analyses

Isotopes are atoms with the same number of protons and electrons, differing only in the numbers of neutrons. The difference in neutron quantity results in different atomic mass and maintenance of the same atomic number. The so called stable isotopes are those that do not decay, that is to say, they are not radioactive. Sulzman (2007) consider that when the number of neutrons and the number of protons are quite similar, the isotope tends to be stable. In contrast, isotopes that derivate from decay are named as radiogenic isotopes.

Generally the isotopic differences between materials are exceedingly small (SULZMAN, 2007), thus an internationally accepted expression comparing to standards is used as represented by the equation below, where xx is the atomic mass of the isotope, E is the element and R is the ratio. As the difference is so small, it is multiplied by one thousand, attributing  $\delta$  values in parts per thousand (ppt - ‰) (DAWSON and SIEGWOLF, 2007).

$$\delta^{xx}E = (R_{\text{sample}}/R_{\text{standard}} - 1) \times 1000$$

Dawson and Siegwolf (2007) point out diverse applications of stable isotope analyses for ecological research, recording and tracing various changes to the earth's diverse terrestrial, aquatic, marine and atmospheric systems. In sedimentary geology, Banner (2003) indicate applications for tracing the sources and transport of dissolved and detrital constituents; reconstruction of temporal changes in ocean water chemistry; and dating the time of formation of rocks and minerals. The use of radiogenic and non-radiogenic isotopes studies done in various disciplines (chemistry, geochemistry, geology, ecology, biology) affirms this methodology as being relevant for environmental science researches.

#### 3.3.1 Isotopic data on paleoclimate and environmental science

The importance of isotopic data for paleoclimate research is evident from long data. Bowen (1988) shows the importance of oxygen and hydrogen fractionation as different isotopic molecules of water into studying the atmosphere and hydrosphere. Those primordial studies showed that continent water is enriched with light stable isotopes in comparison to average oceanic water, thus presenting negative  $\delta^{18}\text{O}$  and  $\delta\text{D}$  values. Therefore, an example could be the formation of the Antarctic ice sheet during the

Miocene epoch increased  $\delta^{18}\text{O}$  registered in benthonic foraminifera, coinciding with sea water isotopic composition.

The “Burke curve” presented on Burke et al (1982), is the secular Sr isotope curve for oceanic water covering the Phanerozoic eon, constructed from analyses of marine carbonates, evaporates and phosphate samples. It reveals systematic temporal variation of seawater strontium composition through geological time (fig. 4). Sources of rocks with low or high strontium ratios influence directly the ratio of carbonates during diagenesis, developing different ratios than the marine original one. This publication intrigued the Earth science community with its potential applications to stratigraphic correlation, diagenesis and fluid flow, paleotectonics, and paleoenvironmental change (BANNER, 2003)

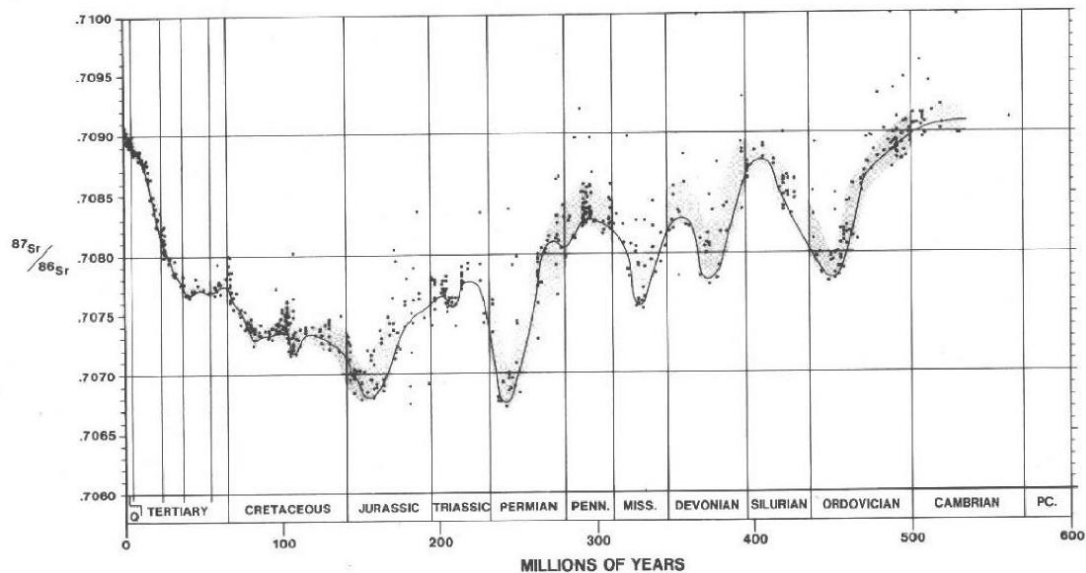


Figure 4- The curve of  $^{87}\text{Sr}/^{86}\text{Sr}$  versus geologic time. The configuration of the curve is strongly influenced by the history of plate interactions and seafloor spreading throughout the Phanerozoic. Source: Burke et al., (1982).

On the other hand, climatic changes were also studied on land, in the beginning by the assessment of the oxygen isotope compositions of  $\text{CaCO}_3$  speleothems and in shells as well as in mammalian and fish bones of calcium phosphate (BOWEN, 1988). In recent years, Sulzman (2007) shows that the field of stable isotopes has grown intensively, becoming almost a standard tool for natural scientists studying element or material cycling in the environment. The easier access to mass spectrometry analysis and the decrease on prices also helped the popularization of isotopic studies. Banner (2003)

summarizes that radiogenic isotope variations in oceans offers unique insight into crustal evolution, weathering, climate change and a range of other Earth surface processes.

### 3.3.2 The Strontium Isotopes

Strontium is an alkaline earth element (symbol = Sr), with atomic number 38, widely distributed on Earth (abundant in seawater, low concentrations for mantle derivate rocks - basic rocks - and highly concentrated in reworked rocks). The element has a ionic radio of about 1.18 Å, therefore can easily substitute for calcium in mineral lattices. In aqueous solution it occurs commonly in the valence Sr(II). This element has four different isotopes, their masses and relative abundance is shown on table X. The  $^{86}\text{Sr}$  isotope is a non-radiogenic isotope, whereas the  $^{87}\text{Sr}$  isotope is produced by the radioactive  $\beta$  – decay of  $^{87}\text{Rb}$  (half-life approx.  $48.8 \times 10^9$  year and decay constant  $\lambda = 1.42 \times 10^{-11}$  year $^{-1}$ ). A  $\beta$  decay is represented by a nuclear reaction where a neutron becomes a proton with the emission of an anti-neutrino and an electron.

Table 1 - The four strontium isotopes, their masses and relative abundance in nature.

<b>Sr Isotopes</b>				
Masses	84	86	87	88
Abundance (%)	0.56	9.87	7.04	82.53

Different from oxygen or hydrogen, Sr isotope ratios are not expressed in standard delta notation, but instead as the ratio of  $^{87}\text{Sr}$  to  $^{86}\text{Sr}$  in a sample. Dawson and Siegwolf (2007) attempt to the importance of understand that the  $^{87}\text{Sr}/^{86}\text{Sr}$  ratio depends on the Rubidium content in the source, and how long ago in time it fractionated from the  $^{87}\text{Rb}$  parent isotope to the  $^{87}\text{Sr}$  daughter isotope. As example of this “Rb - source” on the strontium ratio, the authors show that rocks derived from the Earth’s mantle have low  $^{87}\text{Rb}/^{86}\text{Sr}$  while recent oceanic islands like Hawaii present slightly higher values. With melting of the mantle, Rb isotopes are released into the melt phase with other incompatible elements, so that continental rocks derived from mantle melts present higher  $^{87}\text{Rb}/^{86}\text{Sr}$  ratio, and if reprocessed (weathering releases Sr from certain minerals), it present usually much higher ratios values.

The evolution of the Earth’s crust and mantle related to Sr ratio is summarized by Banner (2003) in four stages. The early Earth, represented by the composition of old meteorites, had very low  $^{87}\text{Sr}/^{86}\text{Sr}$  values ( $\sim 0.699$ ). Mantle-derived igneous rocks of the

upper mantle present low present-day  $^{87}\text{Sr}/^{86}\text{Sr}$  values ( $\sim 0.703$ ). Partial melting and crystal fractionation processes caused higher Rb/Sr, generating heterogeneity on the crust geochemistry reflecting the wide range of magmatic, sedimentary and metamorphic processes. The combined inputs of  $^{87}\text{Sr}/^{86}\text{Sr}$  from crustal material and mantle rocks gave intermediate values for Phanerozoic seawater, reflecting the mixing of the sources in agreement with the high mixing time of ocean waters.

Variations in the Sr isotopic composition are therefore caused entirely by the mixing of Sr derived sources. For this reason, the  $^{87}\text{Sr}/^{86}\text{Sr}$  ratio can be used to identify and quantify the contribution of different Sr sources in a system. In the modern geochemical cycle for Sr, oceanic water is enriched in radiogenic Sr by the weathering of crustal rocks, principally differentiated rocks that are transported to the oceans by superficial rivers or underground water. Low radiogenic ratios sources are the mantle-derived rocks, poorly differentiated, provided from hydrothermal circulations or seafloor rocks. Therefore, variance in the Sr isotopic composition of sea water (fig. 4) can be understood in response to geological events. Periods of seafloor spreading releases lower Sr ratios and orogeny events provide sources of higher Sr values.

In relation to the Sr source in a karst system, Banner (2003) consider the major control as weathering and transport of Ca since Sr follows Ca in its low-temperature aqueous geochemistry and substitute Ca in mineral structures, in this case the stalagmite. Carbonate dissolves directly into solution liberating Sr ions. Weathering reactions produce residual clay minerals that will also introduce new Sr into solution.

Because of the slight mass ratio between Sr isotopes and due to the fact of not occurring in molecule form, biological and chemical processes in nature causes neglected isotopic fractionation (change in the isotopic composition due to chemical/physical process). Halicz et al (2008) also showed that among diverse marine and terrestrial carbonate material, no substantial fractionation in stable strontium isotope composition is observed.

On the other hand, fractionation in the MS is relevant; thereafter the ratio  $^{86}\text{Sr}/^{88}\text{Sr}$  is used to correct this fractionation. The ratio is normalized to a known absolute  $^{88}\text{Sr}/^{86}\text{Sr}$  value (fig. 5) following the equation (2) where  $\beta$  (the fractionation factor) is obtained from equation (1) calculated from known isotopic masses, fixed absolute value (stable 88/86 ratio) and measured (fractionated) ratio (KRABBENHÖFT, 2011).

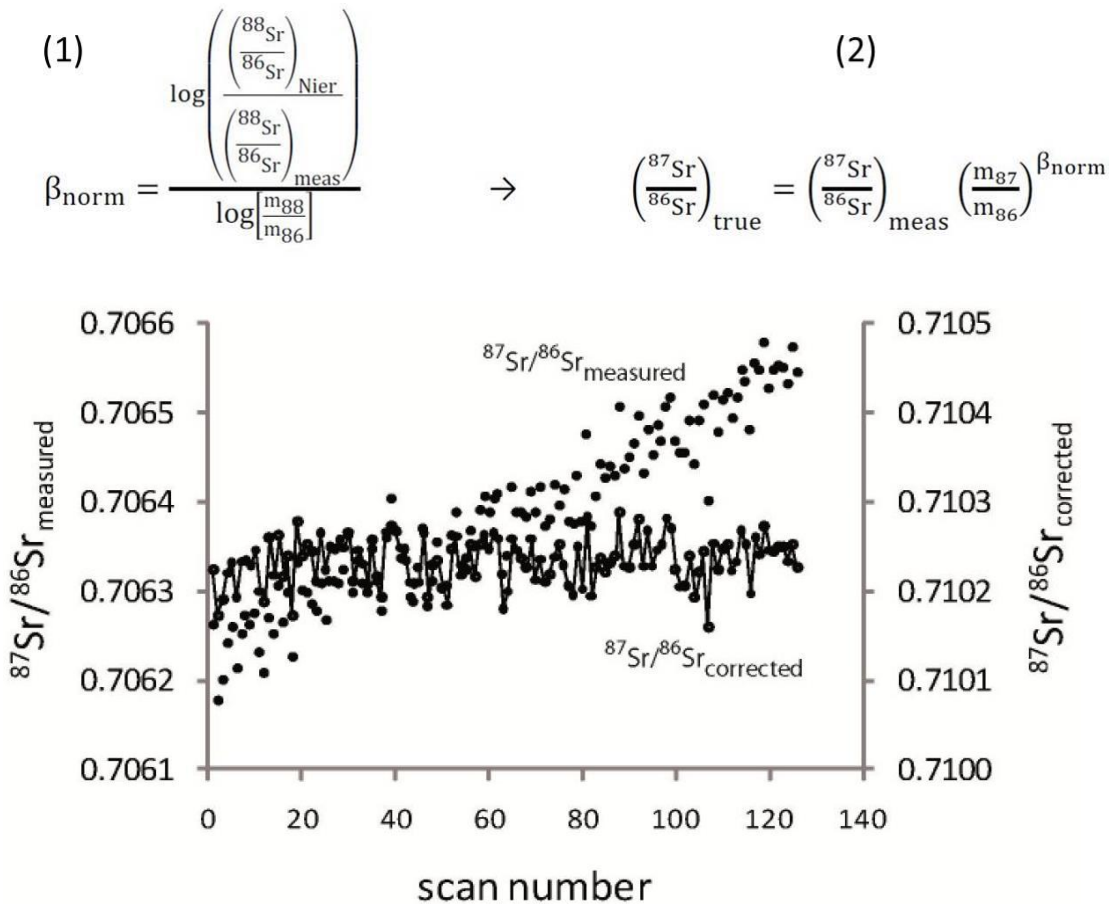


Figure 5- Graphic representation of the fractioning correction normalizing the measured ratio to a fixed absolute  $^{88}\text{Sr}/^{86}\text{Sr}$  value. Source: Nier, (2011).

For the present thesis it was normalized to a standard SRM 987, with nominal  $^{87}\text{Sr}/^{86}\text{Sr} = 0.710248$ . The correction must be done on the varying measured ratios. The variance is generated in the source of the TIMS, where the metal filament is heated, and the light isotopes evaporate easily in comparison with the heavy ones, converting to gas phase. As the source becomes enriched on heavier isotopes during measurement, a variance is noted on the results without fractionation corrections.

## 4 METHODOLOGY

For strontium analysis, initially chemistry separation and concentration of the element is performed by chromatography and then the measurement of isotopes by Mass-Spectrometry device. All samples were homogenized, purified and concentrated before measurement, with special methods described below.

Milli-Q water is used during the chemistry process, and it needs to be completely free of Strontium in a way that no contamination in the original samples is generated. Hence blanks were processed to evaluate potential Sr added by the chemistry process.

All samples were processed at the Institute of Environmental Physics, Heidelberg University. The source of samples and description of the equipment are presented below.

### 4.2 Source of the Samples

The samplings were made by collaborating team of the Institute for Geology, Mineralogy and Geophysics Ruhr-University Bochum, Germany. The stalagmite is from Bunker cave as well the drip water samples (fig. 6).

The soil samples were obtained from a soil profile in the surface just above Bunker cave (51° 22' 03,1" N; 7° 39' 52,9" E) as well as the soil water samples. Sampling was done in two different horizons, the upper – organic A horizon (0,13m) and C horizon (0,75m) with a suction probe UGT (fig. 6).

Meteoric water samples were collected with a rain gauge DIN 58666C on the roof of the German Cave Museum, located 1,5 km west of Bunker cave (RIEHELMANN et al. 2011). A summary list of the samples is shown in Table 2 and a complete list of samples used in this work is presented in Appendix A.

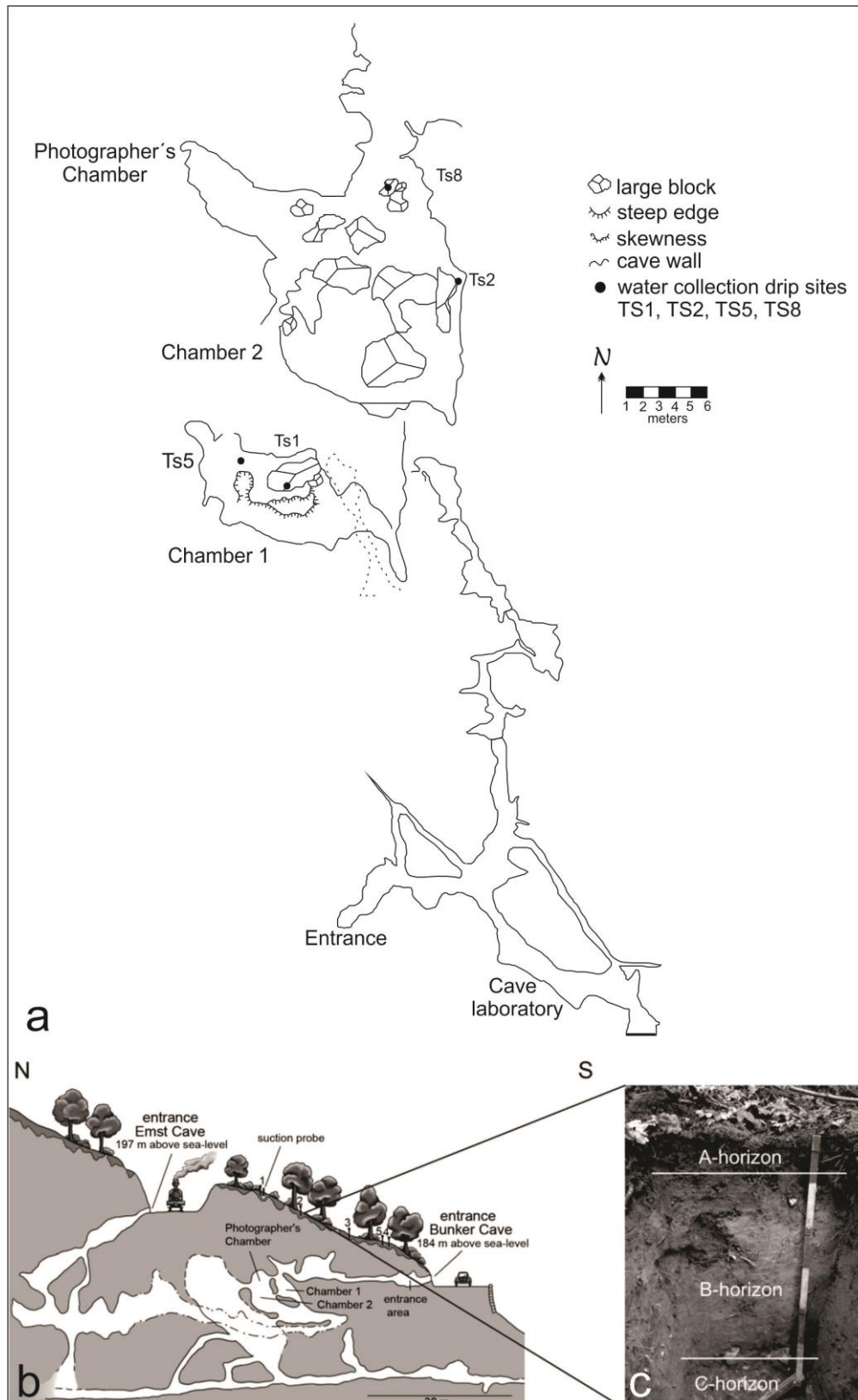


Figure 6- Survey map of the monitoring chambers of Bunker Cave, with indications of the drip sampling sites (a); Longitudinal profile of the cave, showing the monitoring chambers and the soil water sampling site (indicated as suction probe) (b); Soil profile just above the entrance of the cave, where sampling were realized. Modified from Riechelmann et al., (2011).

Table 2: Summary of the samples used in this study, all related to Bunker Cave System.

Sample	Abbreviation name	Quantity of samples	Quantity of analyses	comments
Host rock	HR	2	15	One sample is from the entrance of the cave, containing 2 different layers, one of pure/homogeneous host rock and other from younger carbonate precipitation. The other sample is from an outcrop outside of the cave.
Stalagmite	Bu4	1	8	A complete stalagmite was sampled. For this work were re-sampled from 0,0 (top) up to 14.5 cm of the stalagmite.
Soil	BuS	2	14	Were collected two different horizons of soil: Shallow level (15 cm deep) and deeper level (75 cm deep).
Soil water	SW	4	5	Double sampling (different dates) in the same two points of collect, both above the cave surface.
Drip water	DW	4	4	All collected in Bunker cave in different dripping sites.
Meteoritic water	MW	4	2	Samples collected 1.5 km west from the cave (roof of German cave museum).

### 4.3 Equipment

All solid samples (Bu4, HR and BuS) were powdered and weighted. The powdering of the rock samples (HR and Bu4) was done using a portable dentist drill. All the solid samples (HR, Bu4 and BuS) were weighted using a Mettler Toledo AT261 Delta Range® ISO 9001 balance. The weight measurements were performed in milligram with two decimal places (i.e. 0,01mg).

The liquid samples (MW, DW and SW) were heated forevaporation and concentration using a pack of 3 radiation lamps OSRAM SICCATHERM® E27, with power of 250 Watts. These lamps are used with the aid of suitable holders positioned just above the samples boxes that are connected with a Gerhardt pump. This pump removes the condensed vapor inside the boxes during the evaporation process by suction.

A Thermal Ionization Mass Spectrometer (TIMS) Finnigan Mat MS Model 262 was used for the isotopic measurement, and the standard report was made by the MS Control Program SpectromatRunlt 26 X.

### 4.4 Reagents

Separation of Sr from the calcium matrix was done with TRISKEM resin. The affinity of Sr for the Resin increases with the concentration of nitric acid, with a maximum affinity around 3 and 8 mol L<sup>-1</sup> HNO<sub>3</sub>. Except Sr, other alkali and alkaline earth

elements do not show affinity for the resin (fig. 7). Calcium which is a chemical analogue of strontium shows no affinity to the resin either.

Different concentrations of nitric acid ( $\text{HNO}_3$ ) are used. Purified water ( $18 \Omega \text{ cm}$ ) used through all chemistry is obtained in a Millipore machine, Q-Gard®. Hydrogen peroxide is also used as an anti-organic contamination that could be present in the sample. Due to the high content of particles and compounds in soil, a stronger chemistry procedure take place, with the use of Na-Acetate buffer solution for the dissolution of carbonate content in the sample.

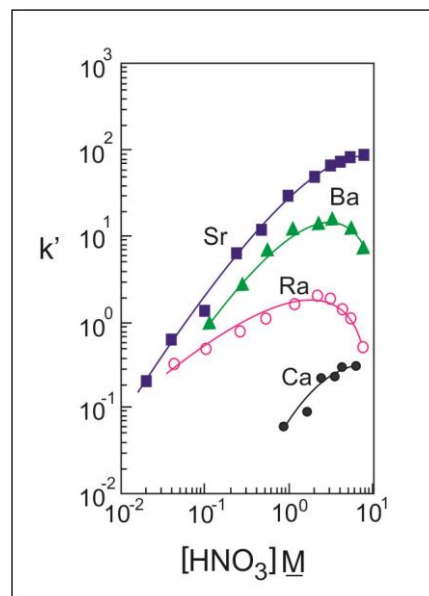


Figure 7- Acid dependency of  $k'$  for various ions at 23-25°C. It is possible to notice that, especially at high nitric acids concentrations, the affinity of the resin for Sr element rise. Modified from Triskem International.

## 4.5 Procedure

### 4.5.1 Rock Samples preparation

Mg and Sr concentrations from previously data (RIECHELMANN et al., 2011) were analyzed to decide where to make the sampling on the stalagmite. Fourteen samples of 2 mg each were made in different high (fig. 8) and numbered according to the laboratory book number (annex 1).

For the HR samples it was chosen a clean and fresh surface of the hand sample, without presence of alteration or weathering. In these conditions four powder samples with 2 mg each, were prepared, being two from the cave entrance and two from outcrops from the

same carbonate unity. The others eleven HR analyses were done by milling 15mg of rock resulting in a very fine gravel (2 to 4 mm). Different grain sizes were used to observe differences in dissolution behavior in relation to exposed surface area.

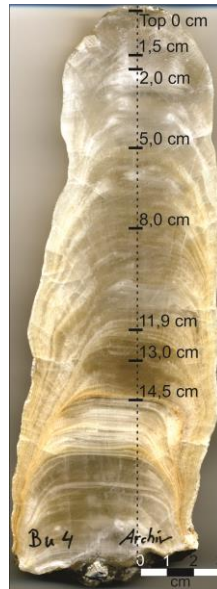


Figure 8- Bu4 stalagmite, with the depth of samples made. The sampling was performed in the principal growth axis (represented by the dashed line).

#### 4.5.2 Soil Samples preparation

In contrast to stalagmites and host rock, the soil samples contain silicates, organic matter, roots, etc. Hence they require chemical treatment to obtain a pure leaching of Sr from the sample for MS measurement. First they are homogenized and organized in small amount.

The first step is to dissolve the carbonate content of the soil, adding to the samples Na-Acetate buffer solution. The reaction occurs with constant shaking and mixing of the buffer solution with the sample, releasing formed  $\text{CO}_2$ . This process may be longer depending on the carbonate content of the sample. The samples are introduced in a centrifuge for 4 minutes with a velocity of 2400 rpm, separating the dissolved carbonate in the liquid phase, decanted and manually separated.

Further the samples are transferred to microwave beakers with  $\text{HCl}_{\text{conc}}$  for total digestion that occurs in the microwave. The next step is to convert into chloride form. The samples are dried under infrared lamps and dissolved, repeating this process three times with different acids. In the first dry cycle the sample is dissolved in concentrated

$\text{HNO}_3$ , in the second cycle in  $9 \text{ mol L}^{-1}\text{HCl}$  and one drop of  $\text{H}_2\text{O}_2$  is also added to avoid oxidation. In the last dry cycle it is dissolved in  $1 \text{ mol L}^{-1}\text{HCl}$ .

The last step is the chromatographic column process for separation of REE (Rare Earth Elements) elements from the soil. The columns are cleaned with Milli-Q water and with  $6 \text{ mol L}^{-1}\text{HCl}$ , and then they are load with Dowex 50 WX 8 and with  $1 \text{ mol L}^{-1}\text{HCl}$ . The samples are poured on the column which is rinse with HCl and eluted the strontium with  $2,5 \text{ mol L}^{-1}\text{HCl}$ .

#### 4.5.3 Water Samples preparation

The water samples are almost ready for the chemistry column process. Reduction by evaporation was done to concentrate the samples. The drip water naturally presents a pure quality, due to the natural filtering process in the karst system, but the meteoric water contain some foreign solid particles that may not enter in the process. Therefore these samples were filtered before the evaporation using a single use filter Sartorius stedimminisart non-pyrogenic with pores of 0,45 microns size.

#### 4.6 Chemistry process

In fig. 9 is observed the flowchart representing the steps of the process. First all samples need to be dissolved in 0.5ml of 3 N  $\text{HNO}_3$  acid. Each sample has one owner column. These column are filled with 0.3 ml of Sr-resin TRISKEM, responsible for retaining the Sr while the others elements are leached. The resin is washed with 6 ml of water, activating the resin. The next step is to activate the resin loading the column with 1ml of  $\text{HNO}_3$  3N and then the sample is loaded.

After the sample loading, the column is washed with 6 ml  $\text{HNO}_3$  in a way that all impurities and other elements go through the column and the strontium is retained in the resin. The elution of the loaded column is done with 3 ml of purified water, and the fluid resulted from this elution is separated in the sample beakers. This final solution (Sr + Milli-Q water) is evaporated and dissolved in a drip of concentrated  $\text{HNO}_3$  and a drip of  $\text{H}_2\text{O}_2$ .

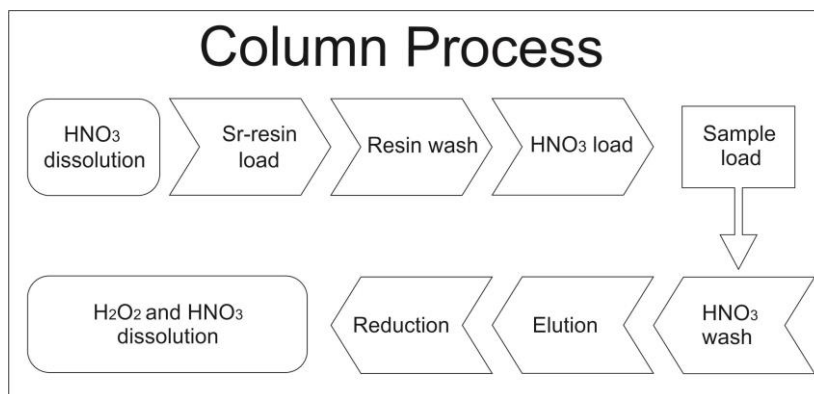


Figure 9- Flowchart representing the chromatographic column process for separating Sr

#### 4.7 Mass spectrometry analyses

The mass spectrometer (MS) is the responsible of separating the different isotopes of interest due to their masses. It is composed basically from an ion source, a magnetic field and detectors. The samples are introduced in the MS by metal filaments (rhenium-filaments) into the ion source. Each sample is added to one filament, and they are arranged always in pairs of sample filament and evaporation filament. (KRABBENHÖFT, 2011).

During the introduction of the sample in the MS, it is necessary to maintain the vacuum inside the equipment. Hence valves between the ion source and the magnetic analyzer are closed due to the maintaining of the vacuum inside the MS. The pressure in the ion source is also controlled, using liquid nitrogen and pumping system after the introduction of the samples. The pressure in the ion source should run around  $3,5 \cdot 10^{-9}$  mbar.

In the ion source the filament (and the sample) are heated by a bombarding of electrons producing positive ions that are accelerated by high voltage into a magnetic field located perpendicular to the ions beam. Passing through this magnetic field the different masses are separated following different paths according to their masses until reach the cups in the detector that were previously positioned according to the paths of the desired isotopes (IAEA, 2001).

In the cups the ions lose their charge emitting electric currents that are amplified and measured by the detector. The measurement obtained in the MS is a result of comparison of different voltages measured in the detector in each cup, related to each

ion beam (each mass, in the case,  $^{88}\text{Sr}$ ,  $^{87}\text{Sr}$  and  $^{86}\text{Sr}$ ). Then, the isotopic ratio is obtained dividing all the isotopes for the stable one ( $^{86}\text{Sr}$ ).

Calibration of the MS is done according to the isotopes to be measured. The calibration is made to rightly positioning of the cups and mathematical corrections of fractionating. According Banner (2003), fractionation can occur in nature or during the analyses, but for strontium isotopes it is clear that the instrumental fractionation is far bigger than natural fractionation, thus the importance of instrumental fractionation correction.

First correction is due the difference behavior of light and heavier isotopes. The light ones are easily evaporated, converting to gas phase in the start of heating in the MS source. This process generates an increase of the molar mass of the residual material in the sample-filament. The second correction is related to the presence of rubidium in the sample. It is corrected by measuring the mass 85, related to rubidium, so the correction of the mass 87 (that correspond even to Sr and Rb) can be done.

Standard sample are used to validate the measurement by a comparison with international laboratory data. The standard material used is the SRM 987.

## 5 RESULTS

The results obtained are isotopic ratios ( $^{87}\text{Sr}/^{86}\text{Sr}$ ) from solid and liquid phases of the karstic profile at Bunker cave (table 3). Sr isotopic ratio are measured in different substracts in the water pathway downwards to the cave ceiling, until the stalagmite formation. The contact of karst water with each of the solid phase elements contribute for a specific geochemical signal in the percolating water, since different ratios were obtained in each material (Appendix A).

Table 3 - Flowchart differing the solid and fluid phases and the sequential stacking materials analyzed, as well as the mean value of its  $^{87}\text{Sr}/^{86}\text{Sr}$  ratios. Notice the lower ratio value for the HR.

Mean (sol. Ph.)	Solid Phase	Flowpath	Fluid Phase	Mean (fl. Ph.)
			Rain	0.7097
0.7101	Soil A		Upper Soil Water	0.7101
0.7089	Soil C	↓	Bottom Soil Water	0.7096
0.7085	Host Rock	↓	Drip Water	0.7094
0.7095	Stalagmite			

Geological material (HR and Bu4) were the mostanalyzed kind of samples, followed by soil leachates. Host rock samples are more abundant and can be sampled not just inside the cave (where implies environmental problems) but also in outcrops on the surface. Soil water could not be sampled during very dry seasons in summer and due to frozen conditions in winter (RIECHELMANN, 2011).

Comparing all the analyzed samples (fig. 10), the HR by far presents the lowest  $^{87}\text{Sr}/^{86}\text{Sr}$  ratio. In agreement, the leachate from C - horizon presents also lower values, since it is an alteration product from HR. The highest ratios values are from horizon A soil water and leachate. As both samples are from the same horizon, it is in agreement that they present similar ratio values. Samples with error above four decimal places were discarded. The stalagmite ratios vary from  $0,709372 \pm 0,000008$  to  $0,709591 \pm 0,000036$ . This range coincides perfectly with drip water ratio, especially with the younger part of the stalagmite (shadow laminasfig. 8).

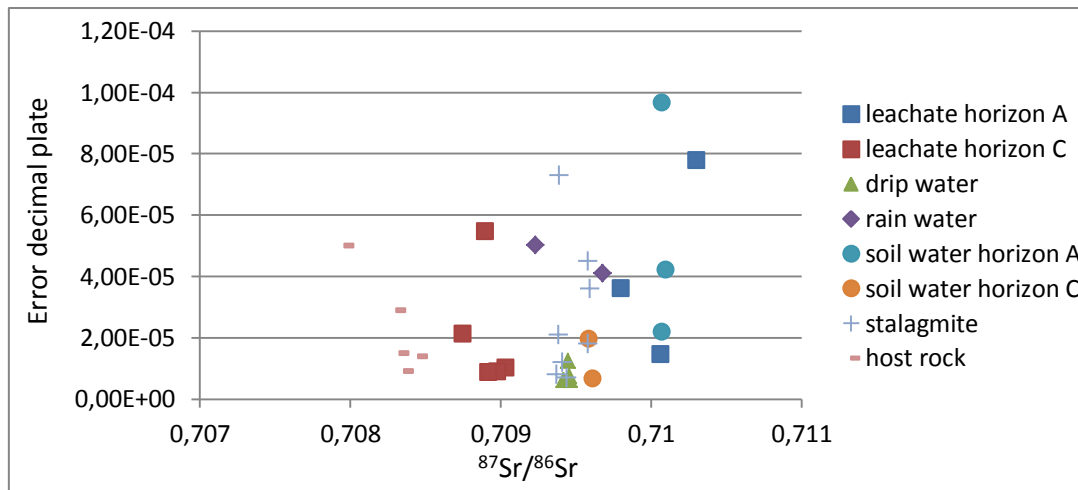


Figure 10- In the horizontal axis is the  $^{87}\text{Sr}/^{86}\text{Sr}$  ratio and in the vertical axis the error values. In the Graphic it is possible to observe the distribution of ratio values from different source samples.

A synthesis of the strontium isotope values for Bunker Cave is shown in fig. 11. Minimum and maximum values, as well mean values are plotted. Soil leachates present the highest values and the host rock the lowest values. The stalagmite isotopic composition is in agreement with the drip water isotopic composition. The biggest arrows, as well as the higher ratios are from soil water, differing considerably from others samples ratio behavior. DW isotopic signal seems to be formed by a mixture of sources, altering the rain signature with soil and rock signals.

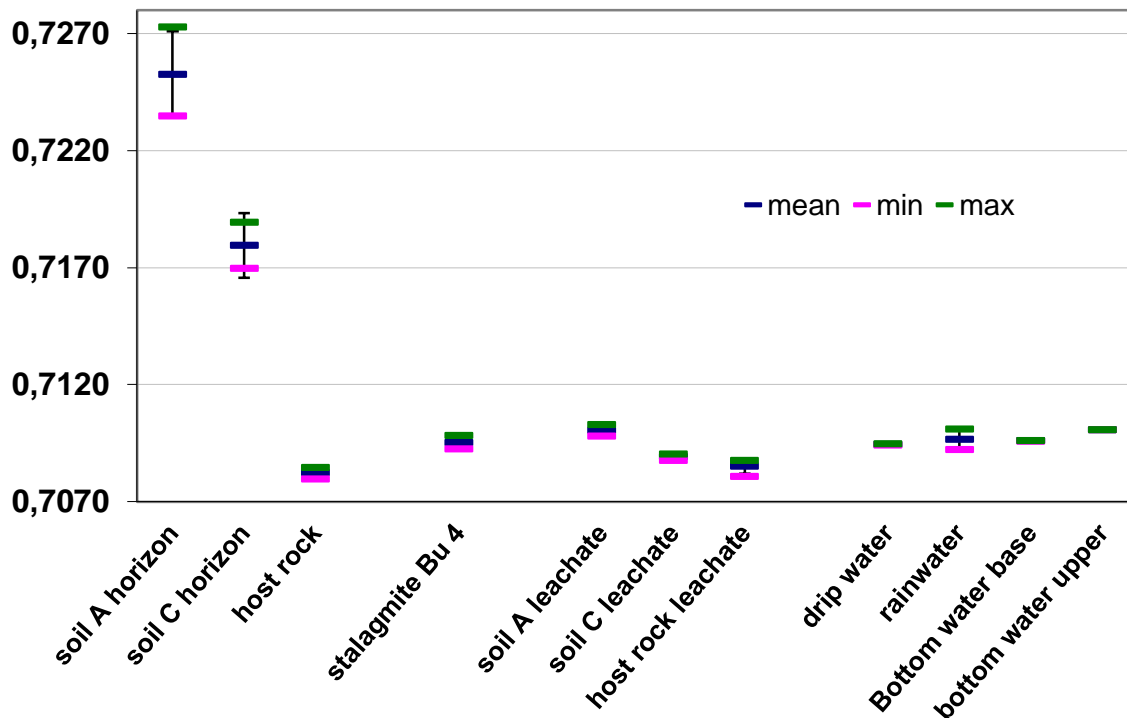


Figure 11- Synthesis diagram with the minimum, maximum and mean values of  $^{87}\text{Sr}/^{86}\text{Sr}$  ratio.

## 5.1 Rain Water

RW samples were filtered due to particles before the concentration process. As concerns to the ratio values, the results are different and unconnected, representing no trend or average between them. In the TIMS, practically no 85 mass was detected, indicating the low Rb content of the RW. The measured values were  $0,7092323 \pm 5,02\text{E-}05$  and  $0,709678 \pm 4,11\text{E-}05$ . The Sr/Ca weight ratio for these samples are 0,00276, higher when compared to other samples due to the low content of Ca in meteoric water (mean value of  $0.9\text{mg/l Ca}^{2+}$  (RIECHELMANN, 2011)).

## 5.2 Soil water and soil leachates

It is clearly distinguishable the signal from A – horizon and C – horizon SW. Upper soil water presents high ratio values, which decreases drastically within the percolation downwards, suggesting an influence of the lower HR ratio. The uniform  $\delta^{18}\text{O}$  values from DW (RIECHELMANN, 2011), indicates a well-mixed karst aquifer. This may influence the abrupt change in the  $^{87}\text{Sr}/^{86}\text{Sr}$  ratio from upper to bottom soil water and not a gradational decreasing trend. The values range between  $0,7095878 \pm 1,95\text{E-}05$  and  $0,7100996 \pm 4,20\text{E-}05$  respectively in base and upper soil horizons (fig. 12).

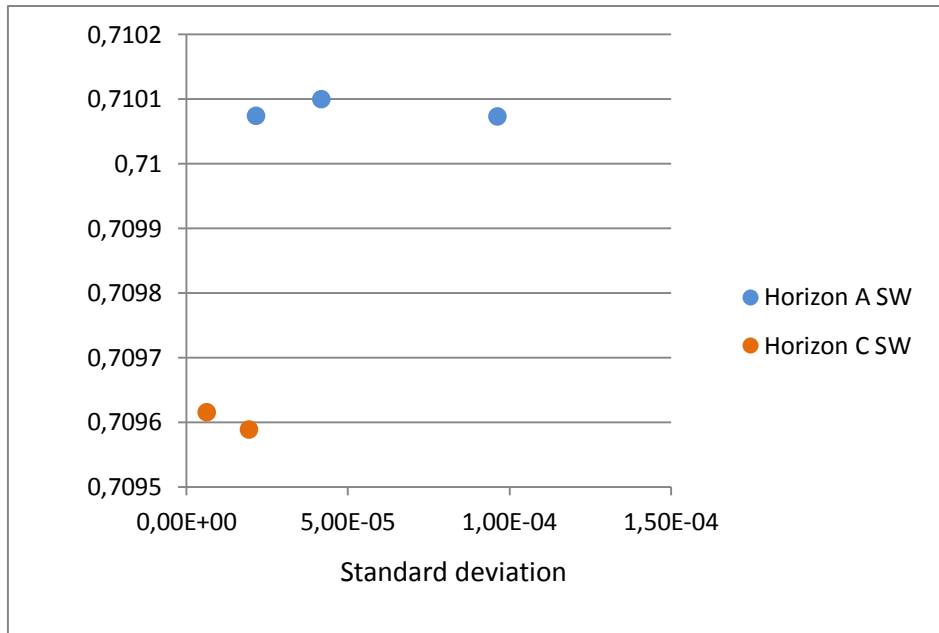
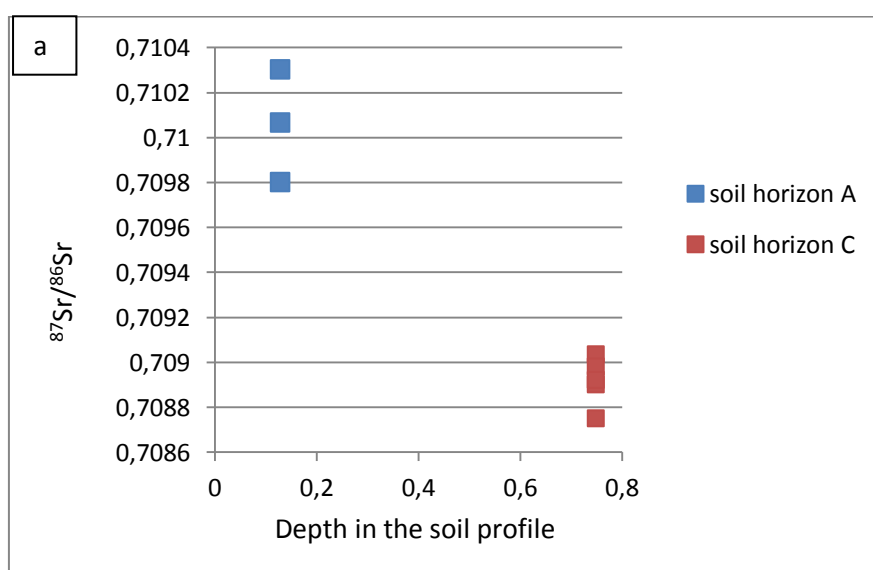


Figure 12 - Soil water samples: Notice the clear different values from the C - horizon soil (lower values) and the upper A - horizon soil samples (higher values).

According to the SW samples, the A-horizon soil leachate presents also higher values as C – Horizon, however the difference is slightly pronounced. All leachates, from different methods (Milli-Q water leach, Na-Acetate leach and HNO<sub>3</sub> leach), presented little differences observed on fig. 13 a. The total digestion of the soil samples resulted in higher values either to upper soil and base soil. The enrichment of A – horizon soil sample with total digestion process is notable (fig. 13 b).



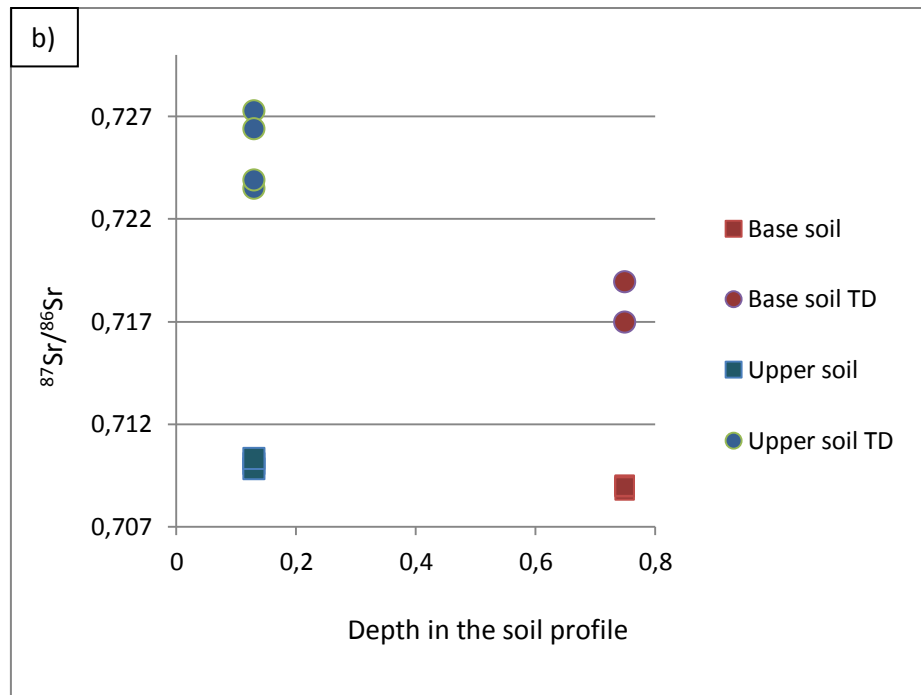


Figure 13- Y axis represent the  $^{87}\text{Sr}/^{86}\text{Sr}$  and X axis the soil depth sampling, 0,13 cm for upper soil and 0,75 cm for base soil. In a) it is shown the higher values of total digestion processes in relation to the simple leachates measurement. In b) it is possible to see the different ratios according to the leachate method used. The difference between lower base soil leachate ratios and higher upper soil leachate ratios is noticeable in both graphics.

### 5.3 Host Rock

The Massif is geologically heterogeneous and that reflects on the geochemistry of the rocks, hence the HR analyzed samples showed also different ratio values. These samples presented the lowest  $^{87}\text{Sr}/^{86}\text{Sr}$  ratios values. No representative difference between outcrop sample ratio and cave entrance ratio was found, even on the re-precipitated calcite layer (fig. 14). 85 mass signals were identified in the TIMS measurement, indicating the presence of some Rb in the HR bulk composition. The strontium ratio values varies between  $0,707960 \pm 5,00\text{E-}5$  to  $0,70845 \pm 1,4\text{E-}05$ .

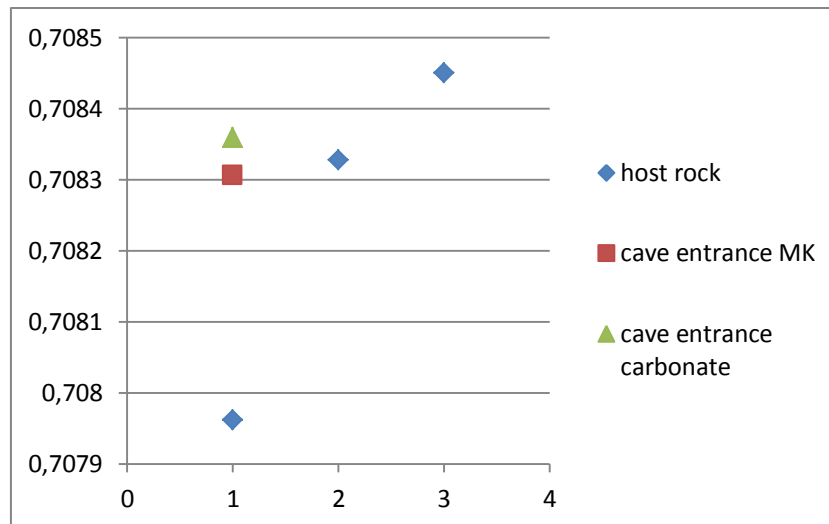


Figure 14- HR  $^{87}\text{Sr}/^{86}\text{Sr}$  ratios.

#### 5.4 Stalagmite and Drip Water

In Bu4 stalagmite eight samples well distributed in the stalagmite axis were analyzed. Dating speleothems as Bu4, it is important to recognize that a drilled sample might contain powders from different time periods (FLEITMANN et al 2008). The sampling of Bu4 was made from ~2 mm diameter cores, perpendicular to the axis in the dated layer. Thus mixing of different ages in relation to age resolution should not be a bigger problem.

In the deeper part of Bu4 (three older samples, fig. 15), the ratio increases significantly, suggesting either that the isotopic composition of the DW changed since then or an enrichment of radiogenic strontium took place in the base of the speleothem during growth time. The lowest  $^{87}\text{Sr}/^{86}\text{Sr}$  ratio of Bu4 (0,709372) is still above from the higher HR ratio (0,70845), in the same way as the  $^{87}\text{Sr}/^{86}\text{Sr}$  data presented by Verheyden et al (2000), suggesting an external source of Sr with a higher isotopic composition than the HR.

As expected, the DW  $^{87}\text{Sr}/^{86}\text{Sr}$  ratios agree well with the stalagmite ratios, with exception of the deeper stalagmite samples due probably to changes in the geochemistry of the percolating water. In respect to A and C horizons leachates, the composition of DW is intermediate, indicating a mixed source (fig.16). This result is in agreement with Wong et al (2011), with lower HR ratios, higher soil leachate values and intermediate DW ratios of the Natural Bridge Caverns in central Texas despite the higher radiogenic

content for all samples in Bunker cave. The  $^{87}\text{Sr}/^{86}\text{Sr}$  ratio from DW varies between the range of  $0,709418 \pm 6,16\text{E-}06$  to  $0,709446 \pm 1,24\text{E-}05$ .

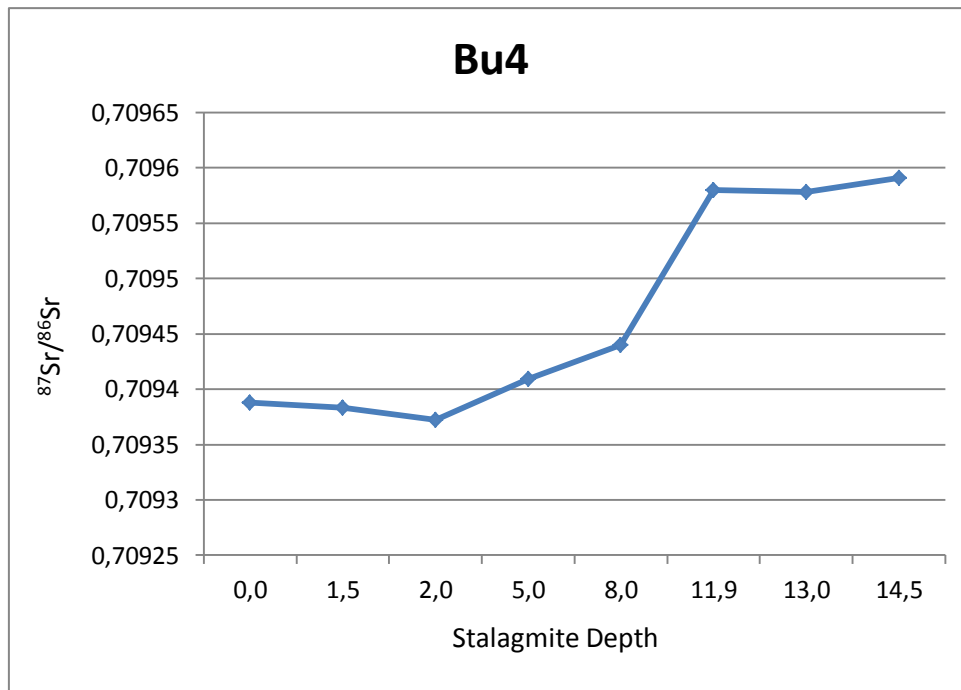


Figure 15-  $^{87}\text{Sr}/^{86}\text{Sr}$  ratio for Bu4 stalagmite. In the X axis is represented the depth of the sample on the stalagmite, starting in the top following to the base. The increasing trend to the base is clear.

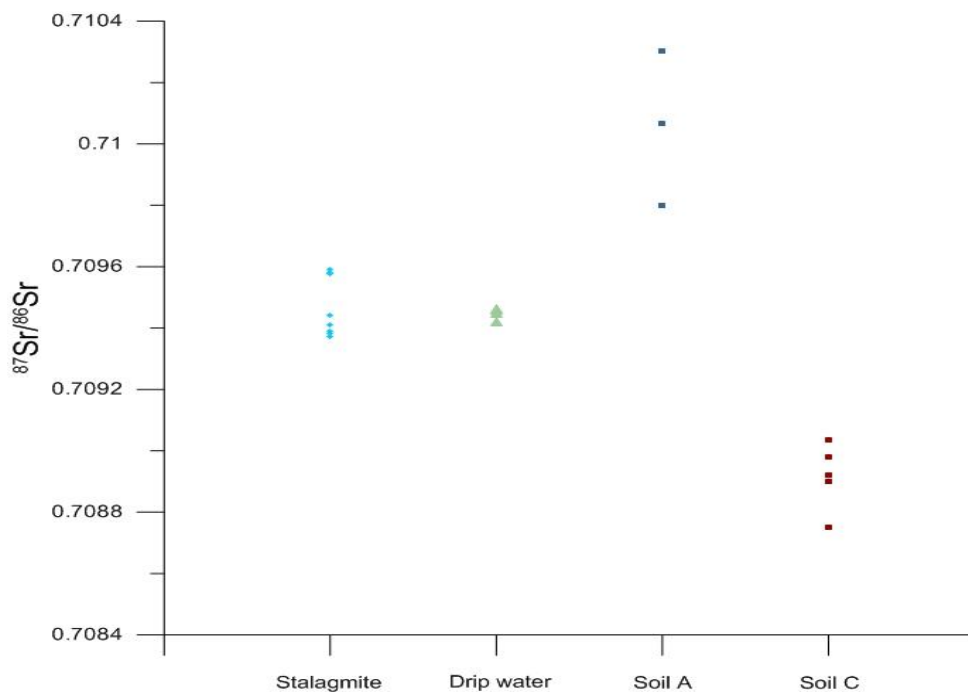


Figure 16- Comparison between  $^{87}\text{Sr}/^{86}\text{Sr}$  ratio from stalagmite, drip water, soil A and soil C. The composition reflects a mixing between the A and C soils horizons ratios.

## 6 DISCUSSION

The rain water presented a mean value ( $^{87}\text{Sr}/^{86}\text{Sr}$ ) of 0.7097, higher than the DW, suggesting that a direct correlation between drip water composition (i.e. stalagmite – the DW signal is reflected directly on the stalagmite) and rain water composition is not established. The interaction of the water through the soil and epikarst prior to the cave ceiling results in variance of the water isotopic composition, due to contribution of different strontium isotopic sources, being the MW ratio not preserved in the system.

The RW should not be also an important source of Sr in the system, due to its low concentrations of Sr. According to Banner (2003) rainwater might present a very low Sr concentration, since Sr is not a volatile element and should remain in the ocean during evaporation. In agreement, Riechelmann (2011) present a mean value of  $3\mu\text{g/l}$  of  $\text{Sr}^{2+}$  in the RW from Bunker cave. Thus the RW does not represent a relevant input of Sr to the system. In contrast, the soil values found suggest the soil to be one of the most important Sr source for the system. Leaching experiments resulted in higher radiogenic ratios, indicating the importance of weathering in the soil to the drip water ratios.

Bunker cave is located approximately 270 km south and 300 km east from the North sea, a quite large distance enough to disregard the effects of sea spray Sr isotopic composition. The Ca content of RW, as affirmed by Banner (2003) may yield insight into the controls of Sr in RW. In the monitoring data base of Bunker cave (Riechelmann 2011), the concentration of  $\text{Ca}^{2+}$  in RW is very low ( $0.9\text{ mg/l}$ ) in agreement. Atmospheric Sr contribution is also negligible according to Drouet et al (2007).

Regarding to the HR composition the mean value obtained (0,7082) is in concordance with the ocean  $^{87}\text{Sr}/^{86}\text{Sr}$  composition presented in the Burke curve (BURKE et al 1982) to the Devonian period that varies between 0,7078 and 0,7086, with a value of 0,7082 to the Late Devonian epoch. In the literature it is well accepted that carbonates register the same Sr composition as the water where there were deposited. The radiogenic ratio can be modified by later diagenesis of the carbonate that seems to be negligible for these carbonate. Very little signal for the 85 mass was measured on the TIMS for the HR, indicating the low content of Rb, as expected for a carbonate rock, composed basically from calcite and some dolomite veins.

The differences between the values of base soil and upper soil are glaring. It is also notable the increasing ratio within the leachates and total digestion processes, due to intensively induced dissolution of soil materials. The high isotopic composition and the considerable Sr content of the soil ( $107\mu\text{g/l Sr}^{2+}$  in soil water, from Riechelmann (2011)) indicates the soil as an important Sr source in the system. The soil is characterized with a low content of clay, rich on silt, as a product from loess loam. This texture classification suggests a considerable porosity that may interfere in the percolation velocity of water and thus in the residence time of Sr in the soil.

The A-horizon is a thin layer, less than 10 cm, and presents the higher ratios (mean value of 0.7253). The contribution of A-horizon to the DW composition may be the most important source of high isotopic composition, that will be slighted by lower signals downwards (soil C and HR) to form the DW final composition deeper in the karst system. It is noteworthy that the uppermost soil is rich in organic matter and siliceous material from dust and surface sediments and approximately 20 % (percentage of the total mass) has clay grain size. This may allow the higher values to A-horizon ratio.

The high radiogenic contribution of erosion and superficial transport of the carboniferous rocks (graywackes and shales) stratigraphically above is not expressive because the river does not anymore flows in the surface (has been captured by the karst) and a vertical flow component predominate actually.

As expected, drip water fits well with stalagmite ratios principally in more recently time, as the deposition of the stalagmite is directly related to the DW chemistry. The greatest amount of radiogenic Sr in the base of the stalagmite reflects a shift in the DW composition. The greatest difference is registered between 12 and 9 cm depth in Bu4, corresponding to  $3.89 \pm 0,16\text{ka}$  and  $2.46 \pm 0,13\text{ ka BP}$  respectively (FOHLMEISTER et al, 2012 – Annex A). This decreasing trend continues slightly until 1.5 cm depth ( $0.83 \pm 0,15\text{ ka BP}$ ) and then turns to a new direction, stopping the decreasing trend and shows a relatively constant values until the top (present – as Bu4 was sampled under an active drip site). In drier conditions, seepage flow predominates, and longer residence time of intense water-rock interaction happens, shifting the DW composition more to the HR values. As comment by Drouet et al (2007), the contrast between the soil source and the HR source is clearly shown in the Sr isotopic records.

Tooth & Fairchild (2003) reinforce that variations in karst drip waters need to have a holistic approach to the karst system to be understood, encompassing atmospheric, soil and aquifer ones. Hydrology exerts a dominant control on water chemistry in terms of both geometry and residence time, both of which determine the degree and characteristics of water-sediment and water-rock interaction.

It is known that in karst aquifers, the water flow has a similar behavior as surface water, and in the same logic, the composition of the water reflect a first-order control by the geology of the regions that they drain (BANNER, 2003). This may suggest that the influence of the HR, with low ratio, is preponderant. However, assuming the actual DW composition, hypothetical end-member contributions represented by the mixing lines (fig. 17) should be ~60% from Soil A ratio and the other ~40% from HR ratio. In this case the biggest contribution is from A horizon, nevertheless, if it is considered the C-horizon formation (fig. 17) this contribution changes to ~40% of Soil A contribution and ~60% of Soil C ratio.

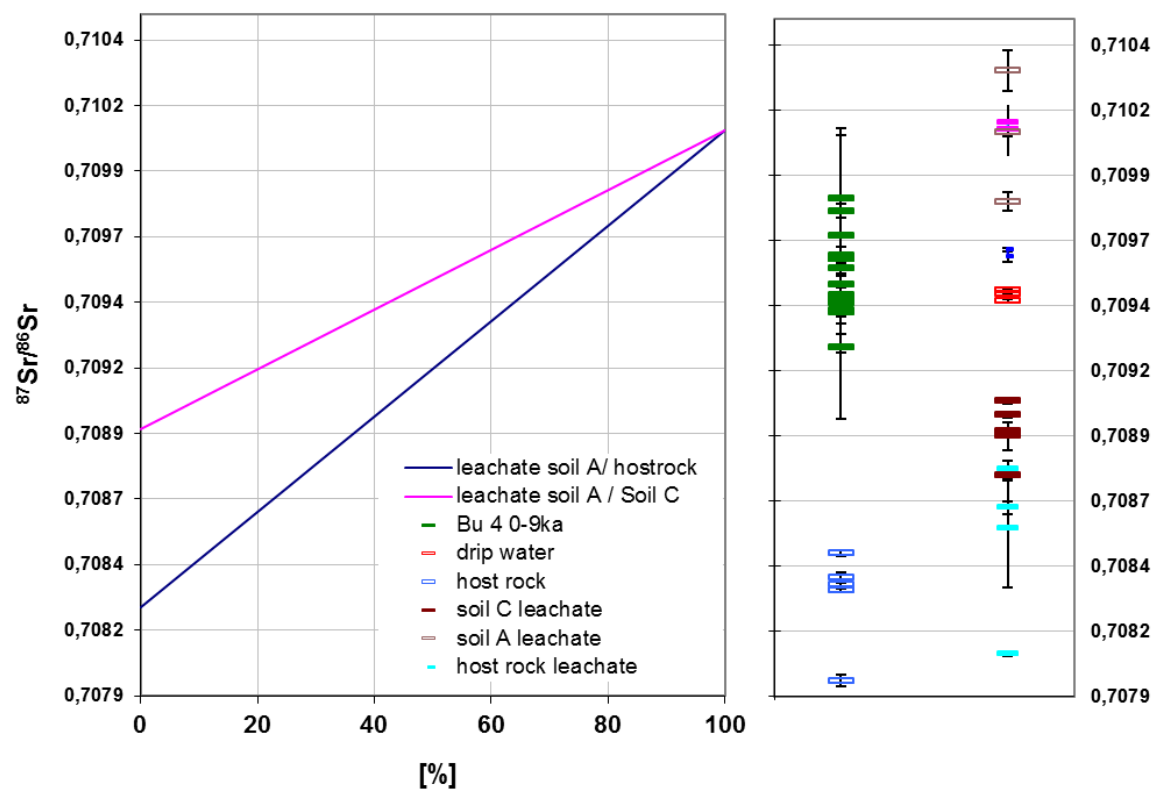


Figure 17-Mixing lines. In the right it is plotted the Sr ratios of the analyzed samples.

Zhou et al (2009) discuss similar mixing lines trying to track Sr sources between two end members. In their case, ~70% of the Sr in the cave water was derived from the HR while the remaining ~30% from the overlying soil layer. The measurement for cave sediment leached by milli-Q water suggests more than 60% of which deriving from the HR. This result shows a larger participation of HR and HR-derived end-member than Bunker cave.

The Bu4 base ratio (~0,7095) has bigger influence of upper soil ratio and Bu4 top ratio (~0,7093) a bigger influence of host rock ratio. The lower  $^{87}\text{Sr}/^{86}\text{Sr}$  ratios in the top of Bu4 can be explained either from (i) more contribution from HR signature or (ii) less contribution from soil A signature or (iii) both simultaneously could result in decrease of the ratio. Verheyden et al (2000) suggest that the radiogenic Sr decrease can be induced by changes in the weathering processes or by differential weathering in the overlying soil. In other hand, an increased input of the low radiogenic Sr can be due to enhanced dissolution of the host rock limestone, but the dissolution of limestone will depend on water availability and acidification of the water. In tropical regions where abundant rainfall occurs and denser vegetation is present generating  $\text{CO}_2$ , the dissolution is more effective (FORD & WILLIAMS, 1996).

If the Sr isotopic composition is a result of mixing between different Sr isotopic compositions, long-term changes in  $^{87}\text{Sr}/^{86}\text{Sr}$  ratios may reflect changes in the relative importance of the two end-members (VERHEYDEN et al, 2000). Clearly it is possible to define 3 end-member sources. Soil A leachate with high ratios, Soil C leachate with slightly low ratios and Host Rock leachate with low values (fig. 16). The DW composition is closer to soil C composition with a mean values difference of only 0,0005, suggesting that the initial fluid with Soil A leachate contribution is altered by a mix of Soil C and HR ratios, promoting the decrease of the ratio of DW in relation to upper soil values.

Following this interpretation, the decreasing trend in the Bu4  $^{87}\text{Sr}/^{86}\text{Sr}$  ratio may suggest a major contribution of soil A leachate in the early Holocene part of the stalagmite (fig. 15). It may be due to the stage of soil evolution. With the uplift of the Massive, and the exposure of the limestone and deposition of later Pleistocene loess over it, started the formation of the soil, where soil transformations and translocations occurred. In the beginning of the soil formation, the weathering input from the rock may be not that

intense as it is for a mature soil profile, inducing the decreasing trend simultaneously with soil profile development.

Perrin (1997, apud VERHEYDEN, 2004) observed an increase the ion concentration in cave waters with increasing cave depth, reflecting the increase in water-rock interaction along time. As longer is the residence time of water in the aquifer, more influence from the HR signal should be attributed to DW ratio. In dryer period, the residence time of water is greater in the epikarst, promoting more dolomite dissolution and increasing the Mg/Ca ratio of the solution. The Sr/Ca ratio covaries with Mg/Ca, providing a major contribution of the HR Sr composition (with lower isotopic ratio). The use of isotopic Sr together with Mg and Sr concentrations in relation to Ca may provide insight to the amount of rainfall.

The shift in the DW composition could also be related to a change in the flow path in the system (i.e. conduit/fracture vs. seepage flow/diffuse). In an initial situation the epikarst is not completely developed and larger fractures may feed Bu4 drip site. With faster flow, there is no much interaction time between HR and water flow necessary to the dissolution of the HR and consequently contribution of Sr ratio from this source. With increasing complexity of the soil profile, a longer flow path through B-Horizon and C-horizon, increased the contact of the percolating water with lower ratios sources, inducing a decreasing trend in the  $^{87}\text{Sr}/^{86}\text{Sr}$  composition of DW in the last 0.85 Ka BP. The hydrological control is extensively discussed in Tooth and Fairchild (2003). They conclude that the soil matrix flow is the dominant karst water source during dry periods.

Extensive literature attribute trends of decreasing  $\text{Ca}^{2+}$  concentrations accompanied by increasing Mg/Ca and Sr/Ca ratios (WONG et al 2011, TOOTH& FAIRCHILD 2003, FOHLMEISER et al., 2012). This co-variation between Mg and Sr in relation to Ca is understand as an effect of PCP (prior calcite precipitation) at lower flow rates, that use to occur in dry periods, when the availability of water is little and ventilated air-filled aquifer porosity is higher.

Prior calcite precipitation is a common process inferred by several authors (ZHOU et al., 2009; WONG et al., 2011; VERHEYDEN et al., 2000; TOOTH& FAIRCHILD 2003; RIECHELMANN et al., 2011; FOHLMEISER et al., 2012). Tooth & Fairchild (2003) explain it as pure calcite precipitated prior to the cave ceiling; due to ventilated air pockets which are not initially in equilibrium with incoming karst water. The

disequilibrium may induce degassing of CO<sub>2</sub> from solution causing the mineral precipitation.

Wong et al (2011) used Sr isotope to discriminate between the effects of water-rock interaction and PCP (prior calcite precipitation). The authors expose that PCP would not alter the <sup>87</sup>Sr/<sup>86</sup>Sr ratio due to the negligible fractionation of Sr isotopes with the degassing of CO<sub>2</sub>, but would rather alter the covering Mg/Ca and Sr/Ca ratios (precipitation of CaCO<sub>3</sub> reduce the Ca<sup>2+</sup> in solution, increasing the amount of this elements in relation to calcium). For Bunker cave, in contrast, a decreasing trend on Mg/Ca ratio within the last 10.8 ka was register by Fohlmeister et al (2012) in comparison to the Sr isotopic data here presented, the <sup>87</sup>Sr/<sup>86</sup>Sr has also a decreasing bias, as well as the Mg/Ca trend, suggesting more effect of the water-rock interaction instead of PCP in the controlling of DW chemistry.

Fairchild et al (2000) interpret shifts in the Sr/Ca and Mg/Ca compositions not for water-rock interaction as Wong et al (2011) rather to selective leaching of Sr and Mg during weathering. In this case, selective leaching of Sr should be marked in increasing <sup>87</sup>Sr/<sup>86</sup>Sr. As Mg/Ca and <sup>87</sup>Sr/<sup>86</sup>Sr have a decreasing trend in Bunker cave, it might not be explained from selective leaching but by longer rock-water interaction (more contribution of HR ratio).

Zhou et al (2009) affirms that speleothem <sup>87</sup>Sr/<sup>86</sup>Sr ratio directly record the Sr isotopic composition of cave water and its variations reflect changes in relative contribution of various Sr sources that have different <sup>87</sup>Sr/<sup>86</sup>Sr signatures in agreement with Bunker cave <sup>87</sup>Sr/<sup>86</sup>Sr ratios here discussed. For them, one of the most important Sr sources for speleothem is the host rock and other significant sources include overlying soil layer, wind-blown dust and sea spray. In the case of Bunker cave, wind-blown dust and sea spray seems to be small or unimportant as to be not worth considering, but a variation between the HR and soil sources seems evident, shifting from a more soil contribution to a more HR contribution during Holocene. This is registered in Bu4 not in a gradational way but with a clear shift in approximately 10 cm deep (~3.35 ± 0.19 ka BP – FOHLMEISTER et al., 2012), possibly indicating a change in the hydrological cycle in the epikarst by this age.

The Sr and <sup>87</sup>Sr/<sup>86</sup>Sr record from Songjia cave (ZHOU et al., 2009) display peak values during the coldest climatic phase and decreased trend after the transition to a warm

period. In Bunker cave the maximum value of  $Bu4$  strontium ratio occurs 14.5 cm deep ( $\sim 5.89 \pm 0.36$  ka BP), an age where Fohlmeister et al (2012) determine a cold and dry period (between 6.5 and 5.5 ka). It may be important to highlight that the environmental conditions in Central China and Central Europe are quite distinct, been the similar results not caused necessarily by the same processes. The effect of intensive rainfall and monsoon behavior of central china reflects in special stalagmites records derived from different process in response to such climatic conditions.

Each proxy type presents a combination of uncertainties that obscures the climate signals of interest (COBB et al., 2008). Such uncertainties must be minimized and a multi proxy approach is able to do it by balancing more evidences in the correlations of different proxies. Fleitmann et al. (2008) also bring to discussion the considerable weakness of speleothem records due to our limited understanding of the true sensitivity of measured parameters to climatic variables. The radiogenic Sr ratio has the potential to increase the discussion (as demonstrated above) on paleoclimate interpretations and thus maximize the potential of high resolution proxy data.

## 7 CONCLUSIONS

The Bunker cave Sr isotope system is here presented. The relevant Sr input sources are soil and host rock. Rain water, sea spray and wind-blow dust as well atmospheric contribution seems not to interfere with the system. The  $^{87}\text{Sr}/^{86}\text{Sr}$  is a good tracer of mixing from different sources. Cave drip water have a isotopic ratio between the host rock and leachates from the overlying soil layer, indicating that Sr in drip water and consequently in the stalagmite is a result of a mixture from different Sr sources.

Three different end-member are defined: Soil A with high  $^{87}\text{Sr}/^{86}\text{Sr}$  ratios, Soil C with slightly low  $^{87}\text{Sr}/^{86}\text{Sr}$  ratios and HR with considerably low  $^{87}\text{Sr}/^{86}\text{Sr}$  ratios. Variations on the strontium isotopic composition suggest changes in the importance of a particular source during specific time. The 87/86 ratio indicated that geology is not the major parameter to influence the drip water composition but more the host rock in interaction with soil profile. The actual drip water isotopic composition is registered ~40% A-horizon and ~60% C-horizon contribution. Naturally, the C-horizon composition depends and correlates directly with host rock alteration.

Bu4 presents a long-term variation on its Sr isotopic ratio, represented by a decreasing trend, marked between 12 and 2 cm deep in the speleothem. The  $^{87}\text{Sr}/^{86}\text{Sr}$  ratio shift is explained as a more prominent water-rock interaction due to longer residence time of water in the epikarst zone during drier periods when seepage flow is dominant. The decreasing trend may be influenced by enhanced contribution of host rock or by a decrease in the A-horizon soil. Both possibilities may occur simultaneously.

Considering increasing input from the host rock it might be possible a correlation with environmental conditions. For enhanced dissolution of the host rock more vegetation activity is necessary to produce  $\text{CO}_2$ , as well abundance of water (rainfall) is needed to dissolve the rock.

PCP does not seem to have an important role in Bunker cave, as opposed to water-rock interaction. The co-varying decrease in  $^{87}\text{Sr}/^{86}\text{Sr}$  and Mg/Ca ratios suggest more host rock contribution. The multi-sample approach in this study is essential to determine from which layer comes the major radiogenic Sr contribution, that might be the same for Mg ions.

In order to interpret climate records from proxies it is necessary to understand how variations of a proxy reflects climate (WONG et al., 2011). As the climate signal from speleothems is filtered in the transit of water through the subsurface, interactions with soil and bedrock do interfere, especially to strontium, indicating other climatic parameters to be analyzed in paleoclimatology research.

## REFERENCES

- AUBRECHT, R.; LÁNCZOS, T.; GREGOR, M.; SCHLÖGL, J.; ŠMÍDA, B.; LIŠČÁK, P.; BREWER - CARIAS, Ch.; VLČEK, L.; 2011. Sandstone caves on Venezuelas Tepuis: Return to pseudokarst? **Journal of Geomorphology**, 132 (2011) 351 – 365.
- BAALES, M.; ORSCHIEDT, J.; STAPEL, B.; Das sauerländische Höhlenland im südlichen Westfalen (Einführung). **Hugo Obermaier-Gesellschaft für Erforschung des Eiszeitalters und der Steinzeit e. V.**, 71 – 74.2011.
- BAKALOWICZ, M.; Karst groundwater: a challenge for new resources. **Hydrogeol Journal, HydroSciences**, 13:148 – 160. 2005.
- BANNER, J. L.; Radiogenic isotopes: systematics and applications to earth surface processes and chemical stratigraphy. **Earth-Science Reviews**, 65: 141-194. 2003.
- BOWEN, R.; Isotopes in palaeoclimatology. In: Bowen R. **Isotopes in the Earth Sciences**. Elsevier Applied Science, 1998. p.: 508 – 526.
- COBB, K.; KIEFER, T.; LOUGH, J.; OVERPECK, J.; TUDHOPE, S.; **Representing and reducing uncertainties in high-resolution proxy climate data**. A report from a workshop sponsored by Electrical Power Research Institute, National Oceanic and Atmospheric Administration, National Science Foundation, International Centre for Theoretical Physics and PAGES/CLIVAR, 2008. Available on: [www.ncdc.noaa.gov/paleo/reports/trieste2008/trieste2008final.pdf](http://www.ncdc.noaa.gov/paleo/reports/trieste2008/trieste2008final.pdf) . Assessed on May/2013.
- DAVIS, W. M.; The Origin of Limestone Caverns. **Science**, New Series, Vol. 73, No. 1891: 327 – 331. 1931.
- DAWSON, T. E. & SIEGWOLF, R. T. W. Using Stable Isotopes as Indicators, Tracers, and Recorders of Ecological Change: Some Context and Background. In: DAWSON, T. E. & SIEGWOLF R. T. W. (editors) **Stable isotopes as indicators of Ecological Change**. Elsevier Academic Press, First edition, 2007 p.: 3 – 18.
- DREYER, R.; NIGGEMANN, S.; RICHTER, D.K.; RIECHELMANN, D.F.C.; Field trip PRE6: Groundwater table caves: quaternary cave systems in the north eastern Rhenish Slate Mountains (Germany). In: **Excursion guidebook – 26<sup>th</sup> IAS Regional Meeting/SEPM-CES Sediment Meeting**, Bochum, Germany, H. 237, 2008, 35-47.
- DROUET, T.; HERBAUTS, J., DEMAIFFE, D.; Change of the Origin of Calcium in Forest Ecosystems in the Twentieth Century Highlighted by Natural Sr Isotopes. In: Dawson T. E. & Siegwolf R. T. W. (editors) **Stable isotopes as indicators of Ecological Change**. Elsevier Academic Press, First edition, 2007p.: 333 – 343.
- EHLERINGER, J. R. & CERLING, T. E. C3 and C4 Photosynthesis. In: MUNN, T. **Encyclopedia of Global Change**. Wiley & Sons, Ltda, Chichester, 2002. pp. 186-190.
- FAIRCHILD, I.J. & BAKER, A. **Speleothem science: From process to past environments**. Oxford: Blackwell publishing, 2012. 420 pp.
- FAIRCHILD, I.J.; BORSATO, A.; TOOTH, A.F.; FRISIA, S.; HAWKESWORTH, C.J.; HUANG, Y.; McDERMOTT, F.; SPIRO, B.; Controls on trace element (Sr-Mg) compositions of carbonate cave waters: implications for speleothem climatic records. **Chemical Geology**, 166:255-269. 2000.
- FLEITMANN, D.; TREBLE, P.; CRUZ Jr., F.; COLE, J.; COBB, K.; **White Paper on “Speleothem-based climate proxy records”**. NOAA Paleoclimatology Reports and Publications, 2008. Available on: [www.ncdc.noaa.gov/paleo/reports/trieste2008/speleothems.pdf](http://www.ncdc.noaa.gov/paleo/reports/trieste2008/speleothems.pdf) . Assessed on: December/2012.
- FOHLMEISTER, J.; SCHRÖDER-RITZRAU, A.; SCHOLZ, D.; SPÖLT, C.; RIECHELMANN, S.; IMMENHAUSER, A.; RICHTER, D.K.; MANGINI, A. Bunker Cave Stalagmites: an archive for central European Holocene climate variability. **Climate of the Past Discussions**, 8, 1687–1720.

2012.

FORD, D. & WILLIAMS, P. **Karst Geomorphology and Hydrogeology**. London: Chapman & Hall publishing, 1996. 601 pp.

FRANKE, W.; The mid-European segment of the Variscides: tectonostratigraphic units, terrane boundaries and plate tectonics evolution. In: FRANKE, W.; HAAK, V.; ONCKEN, O.; TANNER, D.; (eds.) **Orogenic processes: quantifications and modeling in the variscan belt**. Geological society, London, Special Publications, 2000. 179: 35 – 71.

GONÇALVES, F.; RODET, J.; OLIVEIRA, D. C.; MAGALHÃES Jr., A. P.; Cavidades em granitos no município de Santa Maria Madalena – RJ (Brasil). In: **Anais do 31º Congresso Brasileiro de Espeleologia**, Sociedade Brasileira de Espeleologia, 2011. disponível em: [http://www.cavernas.org.br/anais31cbe/31cbe\\_087-093.pdf](http://www.cavernas.org.br/anais31cbe/31cbe_087-093.pdf)

HALICZ, L.; SEGAL, I.; FRUCHTER, N.; STEIN, M.; LAZAR, B.; Strontium stable isotopes fractionate in the soil environments? **Earth and Planetary Science Letters Journal**, 272 : 406-411. 2008.

HARDT, R.; RODET, J.; FERREIRA, S. A. P.; O carste. Produto de uma evolução ou processo? Evolução de um conceito. **Revista de Geografia**, UFPE – DCG/NAPA, v. Especial VIII SINAGEO, n 3. 2010.

HEIN, U. F.; Synmetamorphic Variscian siderite mineralization of the Rhenish Massif, Central Europe. **Mineralogical Magazine**, V. 57, pp. 451-467. 1993.

KLIMCHOUCK, A.; The Formation of Epikarst and Its Role in Vadose Speleogenesis. In: KLIMCHOUCK, A. B.; FORD, D.C.; PALMER, A.N.; DREYBRODT, W.; (eds.) **Speleogenisi: Evolution of Karst Aquifers**. National Speleological Society, Inc., Huntsville, Alabama, U.S.A., 2000. p.: 91 – 99.

KRABBENHÖFT, A.; **Stable Strontium Isotope ( $\delta^{88/86}\text{Sr}$ ) Fractionation in the Marine Realm: A Pilot Study**. 2011. 128 P. Doctor Thesis, der Mathematisch-Naturwissenschaftlichen Fakultät der Christian-Albrechts-Universität zu Kiel. 2011.

KRANJC, A.; About the Name Kras (Karst) in Slovenia. In: 13<sup>th</sup> International Congress of Speleology, 4<sup>th</sup> Speleological Congress of Latin America and Caribbean, 26<sup>th</sup> Brazilian Congress of Speleology. **Anais from the 26<sup>th</sup> Brazilian Congress of Speleology**. Available in: [http://www.cavernas.org.br/anais26cbe/26CBE\\_517-519.pdf](http://www.cavernas.org.br/anais26cbe/26CBE_517-519.pdf)

MEYER, H.; HETZEL, R.; STRAUSS, H.; Erosion rates on different timescales derived from cosmogenic  $^{10}\text{Be}$  and river loads: implications for landscape evolution in the Rhenish Massif, Germany. **International Journal of Earth Science**, 99: 395 – 412. 2010.

MONTEIRO, R. C. & RIBEIRO, L. F. B.; Espeleogenese de cavernas areníticas: algumas considerações aplicadas a Província Espeleológica da Serra do Itaqueri, Estado de São Paulo, Brasil. In: 13<sup>th</sup> International Congress of Speleology, 4<sup>th</sup> Speleological Congress of Latin America and Caribbean, 26<sup>th</sup> Brazilian Congress of Speleology. 2001 Disponível em: [http://www.sbe.com.br/anais26cbe/26CBE\\_129-137.pdf](http://www.sbe.com.br/anais26cbe/26CBE_129-137.pdf)

NIER, A.O.; The isotopic constitution of strontium, barium, bismuth, thallium and mercury. **Physical Review**. 5: 275-279. 1938.

NIGGEMANN, S.; RICHTER, D. K.; VOIGT, S.; WEBER, H-W.; Karst und Höhlen im devonischen Massenkalk der Umgebung von Hagen/Iserlohn (Exkursion N am 29. März 2008). **Jahresberichte und Mitteilung des Oberrheinischen Geologischen Vereins**, N.F. 90: 401 – 434. 2008.

NRCS – Natural Resources Conservation Service. **The Twelve Orders of Soil Taxonomy**. Available in [http://soils.usda.gov/technical/soil\\_orders/](http://soils.usda.gov/technical/soil_orders/). Accessed in 25/05/2013.

RIEHELMANN, D. F.; SCHRÖDER-RITZRAU, A.; SCHOLZ, D.; FOHLMEISTER, J.; SPÖTL, C.; RICHTER, D. K.; MANGINI, A.; Monitoring Bunker Cave (NW Germany): A prerequisite to interpret geochemical proxy data of speleothems from this site. **Journal of Hydrology**, 409 (2011) 682-695. 2008.

RODRÍGUEZ, V. M.; Caracterización de cavidades de bloques graníticos y cuevas estructurales de Vigo-Tui, (Galicia – España). Análisis morfo-estructural del sistema de O Folón. **Cadernos Lab. Xeolóxico de Laxe**, Vol. 28, pp. 231 – 262. 2003.

SAUER, D. & FELIX-HENNINGSSEN, P.; Saproliite, soils, and sediments in the Rhenish Massif as records of climate and landscape history. **Quaternary International**, 156-157:4-12. 2006.

STEENWINKEL, M. V.; The Devonian-Carboniferous Boundary: Comparison between the Dinant Synclorium and the northern border of the Rhenish Slate Mountains: A sequence stratigraphic review. *In: Annales de la Société géologique de Belgique*, T. 115, fasc. 2, 1992, pp. 665 – 681.

SULZMAN, E. W.; Stable isotope chemistry and measurement: a primer. In Michener R. and Lajtha K. **Stable Isotopes in Ecology and Environmental Science**. Second Edition, 2007 Blackwell Publishing, p.: 1 – 18.

TOOTH, A. F.; & FAIRCHILD, I.J.; Soil and karst aquifer hydrological controls on the geochemical evolution of speleothem-forming drip waters, Crag Cave, southwest Ireland. **Journal of Hydrology**, 273: 51 - 68. 2003.

TRISKEM INTERNATIONAL. **Sr Resin**. Available in [http://www.triskem-international.com/en/iso\\_album/ft\\_resine\\_sr\\_en.pdf](http://www.triskem-international.com/en/iso_album/ft_resine_sr_en.pdf). Accessed in 29 November 2012.

VERHEYDEN, S.; KEPPENS, E.; FAIRCHILD, I.J.; McDERMOTT, F.; WEIS, D.; Mg, Sr and Sr isotope geochemistry of a Belgian Holocene speleothem: implications for paleoclimate reconstructions. **Chemical geology**, 169:131-144. 2000.

WAELE, J. D.; PLAN, L.; AUDRA, P. Recent developments in surface and subsurface karst geomorphology: An introduction. **Journal of geomorphology**, 106 (2009) 1 – 8. 2009.

WONG, C. I.; BANNER, J. L.; MUSGROVE, M. L.; Seasonal dripwater Mg/Ca and Sr/Ca variations driven by cave ventilation: Implications for and modeling of speleothem paleoclimate records. **Geochimica et Cosmochimica Acta** 75: 3514 – 3529. 2011.

WRAY, R. A. L.; Opal and Chalcedony speleothems on quartz sandstones in the Sydney region, southeastern Australia. **Australian Journal of Earth Sciences**, 46: 623 – 632. 1999.

ZHOU, H.; FENG, Y.X.; ZHAO, J.X.; SHEN, C.C.; YOU, C.F.; LIN, Y.; Deglacial variations of Sr and  $^{87}\text{Sr}/^{86}\text{Sr}$  ratio recorded by a stalagmite from Central China and their association with past climate and environment. **Journal of Chemical Geology**, 268: 233 – 247. 2009.

## BIBLIOGRAPHY

CRUZ, R. P. D.; **Desenvolvimento de uma metodologia para datação de corais e espeleotemas utilizando o método da razão  $^{230}\text{Th}/^{234}\text{U}$ , por separação cromatográfica e quantificação por espectrometria alfa e FIA-ICP-MS.** 2006. 154 P. Tese de Doutorado, Departamento de química, Pontifícia Universidade Católica do Rio de Janeiro, 2006.

INSERLOHN. Available in: <http://www.iserlohn.de/index.php?id=604> Assessed on 22/05/2013.

KLIMICHOUK, A. B.; **Towards defining, delimiting and classifying epikarst:** Its origin, processes and variants of geomorphic evolution. 2004. Available in [http://speleogenesis.com/directory/karstbase/publication.php?old\\_id=3263](http://speleogenesis.com/directory/karstbase/publication.php?old_id=3263). Accessed in 09 June 2013.

KÜRSCHNER, W.; BECKER, R. T.; BUHL, D.; VEIZER, J.; Strontium isotopes in conodonts: Devonian-carboniferous transition, the northern Rhenish Slate Mountains, Germany. In: *Annales de la Société géologique de Belgique*, T. 115, fasc. 2, 1992. pp. 595 – 621.

OSTER, J.L.; MONTAÑEZ, I.P.; GUILDERSON, T.P.; SHARP, W.D.; BANNER, J.L.; Modeling speleothem  $\delta^{13}\text{C}$  variability in a central Sierra Nevada cave using  $^{14}\text{C}$  and  $^{87}\text{Sr}/^{86}\text{Sr}$ . ***Geochimica et Cosmochimica Acta***, 74:5228-5242. 2010.

RIEHELMANN, D. F. C.; NIGGEMANN, S.; RICHTER, D. K.; SPÖLT, C.; Monitoring Bunker Cave (Sauerland, Germany): preliminary results. ***Geophysical Research Abstracts***, V. 10. 2008.

RIEHELMANN, D. F. C.; SCHRÖDER-RITZRAU, A.; SCHOLZ, D.; SPÖLT, C.; RICHTER, D. K.; MANGINI, A.; Monitoring of Bunker Cave (NW Germany): Assessing the complexity of cave environmental parameters. ***Geophysical Research Abstracts***, V. 12. 2010.

SPÖTL, C.; MATTEY, D.; Scientific drilling of Speleothems – a technical note. ***International Journal of Speleology***, 14(1):29-34. 2012.

URBAN, J.; SCHEJBAL-CHWASTEK, M.; MARGIELWSKI, W.; ZAK, K.; Mineralogical and isotopic (O and C) composition of selected secondary formations in the non-karst caves in sandstones of the Outer Carpathians, southern Poland. In: UIS, 12<sup>th</sup> International Symposium on Pseudokarst, ***Programme and Abstracts***, 2012 p. 14.

**APPENDIX A – SAMPLE LIST**

sample no. TIMS book	sample	sample-dft(cm)	sample weight (mg or ml)	meas. date	mass 85 (mV)	87/86 TE	error	Sr/Ca weight ratio
5669	stalagmite	Bu4-11.9	10,9	23/05/2012		0,70958	4,50E-05	7,94E-05
5670	stalagmite	Bu4-14.5	5,6	24/05/2012		0,709591	3,60E-05	8,40E-05
5673	stalagmite	Bu4-top	-	13/06/2012		0,709427	9,50E-05	7,80E-05
5692	stalagmite	Bu4- 1.5	12,54	20/06/2012		0,709383	2,10E-05	5,57E-05
5693	stalagmite	Bu4- 2.0	12,97	21/06/2012		0,709372	8,00E-06	5,30E-05
5695	stalagmite	Bu4- 5.0	11,96	21/06/2012		0,709409	1,20E-05	7,84E-05
5696	stalagmite	Bu4- 8.0	14,43	22/06/2012		0,70944	7,00E-06	8,16E-05
5697	stalagmite	Bu4- 13.0	13,48	20/06/2012		0,709578	1,80E-05	8,39E-05
5687	Host rock	MK 1	15,48	18/06/2012		0,707962	5,00E-05	1,54E-03
5688	Host rock	Mk 2	13,22	18/06/2012	1 mV	0,708328	1,50E-05	6,77E-04
5689	Host rock	Mk 4	12,95	19/06/2012	1 mV	0,70845	1,40E-05	5,38E-04
5690	Host rock/cave entrance	HE MK	12,58	19/06/2012		0,708306	2,90E-05	3,93E-04
5691	Host rock/cave entrance	HE Ca	13,58	20/06/2012		0,708359	9,00E-06	1,19E-04
5710	drip water	TS 1 7/11	approx. 100ml	06/08/2012		0,70946	6,20E-06	8,44E-04
5711	drip water	TS 8 10/11	approx. 100ml	06/08/2012		0,709418	6,16E-06	1,42E-03
5712	drip water	TS 5 9/11	approx. 100ml	08/08/2012		0,709446	1,24E-05	8,45E-04
5713	drip water	TS 2 4/12	approx. 100ml	07.08.2012 08.08.2012	1000cps 500cps	0,709457	7,42E-06	1,84E-03
5794	Na-Acetat leachate	soil 1; 0,13m 1-1a	99,8	06.08.2012 07.08.2012		0,710066	1,45E-05	4,47E-03
5795	MilliQ leachate	soil 1; 0,13m 1-1b	99,8	08/08/2012		0,7098	3,60E-05	5,28E-03
5798	0,1N HNO3 leachate	soil 1; 0,13m 1-3a	102,4	10/08/2012		0,710302	7,79E-05	4,31E-03
5800	Na-Acetat leachate	soil 4; 0,75m 4-1a	102,3	13/08/2012		0,70875	2,13E-05	4,53E-04
5801	MilliQ leachate	soil 4; 0,75m 4-1b	102,3	13/08/2012		0,7089	5,47E-05	4,90E-04

sample no. TIMS book	sample	sample-dft(cm)	sample weight (mg or ml)	meas. date	mass 85 (mV)	87/86 TE	error	Sr/Ca weight ratio
5802	Na-Acetat leachate	soil 4; 0,75m 4-2a	499,7	14/08/2012		0,709034	1,02E-05	
5803	MilliQ leachate	soil 4; 0,75m 4-2b	499,7	15/08/2012		0,70898	8,84E-06	
5804	0,1N HNO3 leachate	soil 4; 0,75m 4-3a	102	15/08/2012		0,70892	8,60E-06	4,80E-04
5867	total chemical digestion	soil 1; 0,13m 1-1 mit FeMN treating	99,8	22/08/2012		0,727269	7,08E-06	
5868	total chemical digestion	soil 1; 0,13m 1-2 ohneFeMN treating	299,5	22/08/2012		0,7263784	6,79E-06	
5870	total chemical digestion	soil 4; 0,75m 4-2 ohneFeMN treating	499,7	23/08/2012		0,7169696	6,92E-06	
5915	rainwater	RW 7/09	100	17/01/2013		0,709232349	5,02E-05	2,76E-03
5917	rainwater	RW 12/08	100	21/01/2013	sehr wenig	0,709678002	4,11E-05	2,76E-03
5935	bottom water (base soil)	BW 1 4/11	70	21/01/2013		0,709587773	1,95E-05	1,01E-03
5936	bottom water base soil	BW 1 4/12	60	18/01/2013		0,709615302	6,54E-06	1,01E-03
5937	bottom water upper soil	BW 2 2/12	50	17/01/2012		0,710073327	2,18E-05	1,77E-03
5938	bottom water upper soil	BW 2 6/12	50	16/01/2012		0,710072915	9,66E-05	1,82E-03
5938	bottom water upper soil	BW 2 6/12	50	16/01/2012		0,710099597	4,20E-05	1,82E-03
5952	Bu soil 1-1	Bu soil 1-1	144	22/01/2013		0,723473773	3,16E-05	
5953	Bu soil 1-2	Bu soil 1-2	186	22/01/2013		0,723898154	1,67E-05	1,51E-02
5954	Bu soil 4-1	Bu soil 4-1	208	22/01/2013	ja	0,71892909	7,84E-06	6,84E-04

sample no. TIMS book	sample	sample-dft(cm)	sample weight (mg or ml)	meas. date	mass 85 (mV)	87/86 TE	error	Sr/Ca weight ratio
5976	0,1N HNO3 leachate 1	MK1W - 1	14,4			0,708063167	8,74E-06	1,21E-03
5978	0,1N HNO3 leachate 1	MK4 - 1	15,1			0,708625646	2,51E-05	2,86E-04
5979	MilliQ leachate 1	MK4 - 2	15,6			0,708770189	3,57E-05	7,57E-04
5980	host rock	MK1W - 3	3,3			0,708083376	9,41E-06	1,54E-03
5985	0,1N HNO3 leachate 2	MK1W - 1	-			not enough for sufficient measurement		
5986	MilliQ leachate 2	MK1W - 2	-			not enough for sufficient measurement		
5987	0,1N HNO3 leachate 2	MK4 - 1	-			not enough for sufficient measurement		
5988	MilliQ leachate 2	MK4 - 2	-			not enough for sufficient measurement		

\*(n=46) samples with standard deviation larger than 0,0E-5

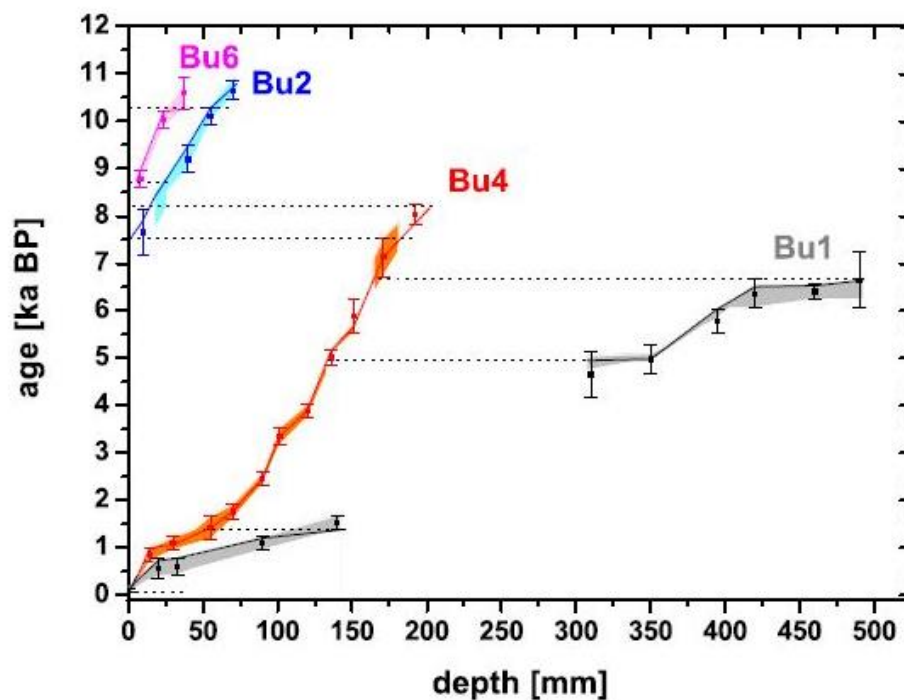
**ANNEX A – BU4 DATING DATA**

Uranium and Thorium isotopic compositions and  $^{230}\text{Th}$  for Bunker Cave stalagmite Bu4 measured by TIMS. Errors are  $2\sigma$  analytical errors. Corrected  $^{230}\text{Th}$  ages assume initial  $^{230}\text{Th}/^{232}\text{Th}$  concentration ratio of  $3.8 \pm 1.9$ .

Sample ID	$^{238}\text{U}$ [ppb]	$^{232}\text{Th}$ [ppt]	$\delta^{234}\text{U}$ [‰]	$(^{230}\text{Th}/^{238}\text{U})$ act. ratio	age <sub>uncorrected</sub> [ka BP]	age <sub>corrected</sub> [ka BP]
<b>Bu4</b>						
Bu4 – 1.45 cm*	66 ± 0.1	54 ± 33	662 ± 24	0.0135 ± 0.0022	0.85 ± 0.15	0.83 ± 0.15
Bu4 – 3 cm	79.5 ± 0.2	47 ± 0	501 ± 7	0.0157 ± 0.0019	1.10 ± 0.14	1.09 ± 0.14
Bu4 – 5.5 cm	75.4 ± 0.2	1881 ± 9	514 ± 7	0.0204 ± 0.0011	1.89 ± 0.08	1.42 ± 0.26
Bu4 – 7 cm	72.0 ± 0.1	590 ± 4	548 ± 7	0.0256 ± 0.0020	1.91 ± 0.14	1.76 ± 0.16
Bu4 – 9 cm	68.6 ± 0.1	227 ± 2	582 ± 8	0.0361 ± 0.0018	2.52 ± 0.13	2.46 ± 0.13
Bu4 – 10.15 cm*	57.7 ± 0.1	592 ± 31	558 ± 10	0.0480 ± 0.0022	3.53 ± 0.16	3.35 ± 0.19
Bu4 – 12 cm	95.8 ± 0.2	390 ± 2	598 ± 7	0.0569 ± 0.0021	3.96 ± 0.15	3.89 ± 0.16
Bu4 – 13.6 cm*	102.9 ± 0.2	1038 ± 27	587 ± 7	0.0724 ± 0.0016	5.20 ± 0.11	5.02 ± 0.15
Bu4 – 15.1 cm*	69.1 ± 0.1	2019 ± 27	664 ± 7	0.0888 ± 0.0034	6.39 ± 0.24	5.89 ± 0.36
Bu4 – 17.1 cm*	69 ± 0.1	1200 ± 41	600 ± 10	0.1027 ± 0.0051	7.45 ± 0.37	7.14 ± 0.41
Bu4 – 19.25 cm*	84.1 ± 0.2	368 ± 30	537 ± 9	0.1103 ± 0.0029	8.11 ± 0.22	8.03 ± 0.23

Source: Fohlmeister et al (2012).

Th/U ages (solid squares) and associated  $2\sigma$  -uncertainties (shaded areas) as well as the age-depth models (solid line) for the four stalagmites from Bunker Cave. The thin dotted lines denote overlapping sections between the four speleothems.



Source: Fohlmeister et al (2012).